Hunga Tonga-Hunga Ha'apai Volcano Impact Model Observation Comparison (HTHH-MOC) Project: Experiment Protocol and Model Descriptions

Yunqian Zhu[1,2], Hideharu Akiyoshi[3], Valentina Aquila[4], Elisabeth Asher[1,5], Ewa M. Bednarz[1,2], Slimane Bekki[6], Christoph Brühl[7], Amy H. Butler[2], Parker Case[8], Simon Chabrillat[9], Gabriel Chiodo[10], Margot Clyne[11,12], Peter R. Colarco[8, 37], Sandip Dhomse[18], Lola Falletti[6], Eric Fleming[8,13], Ben Johnson[38], Andrin Jörimann[10,36], Mahesh Kovilakam[15], Gerbrand Koren[16], Ales Kuchar[17], Nicolas Lebas[14], Qing Liang[8], Cheng-Cheng Liu[12], Graham Mann[18], Michael Manyin[8,13], Marion Marchand[6], Olaf Morgenstern[19,20*], Paul Newman[8], Luke D. Oman[8], Freja F. Østerstrøm[21,22], Yifeng Peng[23], David Plummer[24], Ilaria Quaglia[25], William Randel[25], Samuel Rémy[26], Takashi Sekiya[27], Stephen Steenrod[8,28], Timofei Sukhodolov[36], Simone Tilmes[25], Kostas Tsigaridis[29,30], Rei Ueyama[31], Daniele Visioni[32], Xinyue Wang[11], Shingo Watanabe[27], Yousuke Yamashita[3], Pengfei Yu[33], Wandi Yu[34], Jun Zhang[25], Zhihong Zhuo[35]

1. Cooperative Institute for Research in Environmental Sciences (CIRES), University of Colorado Boulder, USA
2. NOAA Chemical Sciences Laboratory, Boulder, USA
3. National Institute for Environmental Studies, Tsukuba, Japan
4. American University, Department of Environmental Science, Washington, DC, USA
5. NOAA Global Monitoring Laboratory, Boulder, USA
6. LATMOS, UVSQ, CNRS, INU, Sorbonne Université, Paris, France
7. Max Planck Institute for Chemistry, Mainz, Germany
8. NASA Goddard Space Flight Center, Maryland, USA
9. Royal Belgian Institute for Space Aeronomy (BIRA-IASB), Brussels, Belgium
10. Institute for Atmospheric and Climate Science, ETH Zurich, Zurich, Switzerland; Instituto de Geociencias, Spanish National Research Council (IGEO-CSIC-UCM), Madrid
11. Department of Atmospheric and Oceanic Sciences, University of Colorado Boulder, Boulder, USA
12. LASP, University of Colorado Boulder, Boulder, USA
13. Science Systems and Applications, Inc., Lanham, MD, USA
14. LOCEAN/IPSL, Sorbonne Université, CNRS, IRD, MNHN, Paris, France
15. NASA Langley Research Center, VA, USA
16. Copernicus Institute of Sustainable Development, Utrecht University, Utrecht, Netherlands
17. BOKU University, Vienna, Austria
18. School of Earth and Environment, University of Leeds; UK National Centre for Atmospheric Science, University of Leeds, Leeds, UK
19. National Institute of Water and Atmospheric Research (NIWA), Wellington, New Zealand
20. School of Physical and Chemical Sciences, University of Canterbury, Christchurch, New Zealand
21. School of Engineering and Applied Sciences, Harvard University, Cambridge, MA, USA
22. Department of Chemistry, University of Copenhagen, Copenhagen, Denmark
23. Lanzhou University, Lanzhou, China
24. Climate Research Division, Environment and Climate Change Canada, Montréal, Canada

45   25. NCAR ACOM, Boulder, USA
46   26. HYGEOS, Lille, France
47   27. Japan Agency for Marine-Earth Science and Technology (JAMSTEC), Yokohama, Japan
48   28. University of Maryland-Baltimore County, Baltimore, MD, USA
49   29. Center for Climate Systems Research, Columbia University, New York, NY, USA.
50   30. NASA Goddard Institute for Space Studies, New York, NY, USA.
51   31. NASA Ames Research Center, Moffett Field, CA
52   32. Department of Earth and Atmospheric Sciences, Cornell University, Ithaca, NY
53   33. Jinan University, Guangzhou, China
54   34. Lawrence Livermore National Laboratory, USA
55   35. Department of Earth and Atmospheric Sciences, University of Quebec in Montreal, Montreal
56   (Quebec), Canada
57   36. Physikalisch-Meteorologisches Observatorium Davos and World Radiation Center, Davos,
58   Switzerland
59   37. Earth System Science Interdisciplinary Center, University of Maryland, College Park, MD
60   USA
61   38. Met Office Hadley Centre, Exeter, UK
62
63
64   * now at: German Meteorological Service (DWD), Offenbach, Germany
65
66
67   Correspondence to: Yunqian Zhu yunqian.zhu@colorado.edu
68

69   **Abstract:**
70

71   The 2022 Hunga volcanic eruption injected a significant amount of water vapor and a moderate
72   amount of sulfur dioxide into the stratosphere causing observable responses in the climate
73   system. We have developed a model-observation comparison project to investigate the evolution
74   of volcanic water and aerosols, and their impacts on atmospheric dynamics, chemistry, and
75   climate, using several state-of-the-art chemistry climate models. The project goals are: 1.
76   Evaluate the current chemistry-climate models to quantify their performance in comparison to
77   observations; and 2. Understand atmospheric responses in the Earth system after this exceptional
78   event and investigate the potential impacts in the projected future. To achieve these goals, we
79   designed specific experiments for direct comparisons to observations, for example from balloons
80   and the Microwave Limb Sounder satellite instrument. Experiment 1 consists of two sets of free-
81   running ensemble experiments from 2022 to 2031: one with fixed sea-surface temperatures and
82   sea-ice, and one with coupled ocean. These experiments will help to: understand the long-term
83   evolution of water vapor and aerosols; quantify HTHH effects on stratospheric and mesospheric
84   temperatures, dynamics, and transport; understand the impact of dynamic changes on ozone
85   chemistry; quantify the net radiative forcings; and evaluate any surface climate impact.
86   Experiment 2 is a nudged-run experiment from 2022 to 2023 using observed meteorology. To
87   allow participation of more climate models with varying complexities of aerosol simulation, we
88   include two sets of simulations in Experiment 2: Experiment 2a is designed for models with
89   internally-generated aerosol while Experiment 2b is designed for models using prescribed
90   aerosol surface area density. This experiment will help to: analyze H_2O & aerosol evolution;

91 quantify the net radiative forcings; understand the impacts on mid-latitude and polar O_3
92 chemistry as well as allow close comparisons with observations.
93
94 **1. Introduction and motivations of this project**
95
96   The Hunga Tonga-Hunga Ha'apai (HTHH) Impacts activity was established in the World
97 Climate Research Programme (WCRP) Atmosphere Processes And their Role in Climate
98 (APARC) as a limited-term focused cross-activity with a duration of three years. It aims to assess
99 the impacts of the 15 January 2022 Hunga volcanic eruption and produce an assessment to
100 document the Hunga impact on the climate system. The Hunga eruption injected an
101 unprecedented amount of water (H_2O) and moderate sulfur dioxide (SO_2) into the stratosphere
102 (Millan et al., 2022), presenting a unique opportunity to understand the impacts on the
103 stratosphere of a large-magnitude explosive phreatomagmatic eruption. The wide range of
104 satellite observations of the stratospheric water and sulfate plumes, global transport and
105 dispersion of volcanic materials, and unusual chemical and temperature signals are helpful in
106 assessing model representations of stratospheric chemistry, aerosol, and dynamics. For example,
107 the Aura Microwave Limb Sounder (MLS) observed ~150 Tg of water injected by the Hunga
108 eruption (Millan et al., 2022), which slowly decayed due to the polar stratospheric cloud (PSC)
109 dehydration process and stratosphere-troposphere exchange (Fleming et al., 2024; Zhou et al.,
110 2024). Large aerosol optical depth is observed by Ozone Mapping and Profiler Suite (OMPS)
111 (Taha et al., 2022), due to fast formation of sulfate (Zhu et al., 2022) and the high optical
112 efficiency of Hunga aerosol particles (Li et al., 2024). Unlike the stratospheric warming patterns
113 observed from previous large volcanic eruptions (El Chichón in 1982 and Pinatubo in 1991),
114 global stratospheric temperatures decreased by 0.5 to 1.0 K in the first two years following the
115 Hunga eruption, largely due to radiative cooling from injected water vapor (Randel et al., 2024).
116 Satellite observations in June, July, August 2022 reveal reduced lower stratospheric ozone (O_3)
117 over the SH midlatitudes and subtropics, with high levels near the equator, exceeding previous
118 variability. These ozone anomalies coincide with a weakening of the Brewer-Dobson circulation
119 during this period (Wang et al., 2023). Changes in stratospheric winds also influence the
120 mesosphere, leading to a stronger mesospheric circulation and corresponding temperature
121 changes (Yu et al., 2023). These observed phenomena provide a unique opportunity to test the
122 ability of chemistry-climate models to simulate the evolution of volcanic aerosols combined with
123 such a large amount of water vapor, as well as understand how volcanic water vapor and aerosols
124 modify radiative balances and stratospheric ozone.
125   The APARC HTHH Impacts activity aims to provide a benchmark analysis of the
126 eruption impacts so far, and projections of eruption climate impacts over the next few years. Two
127 multi-model evaluation projects are designed to facilitate the success of this activity: Tonga
128 Model Intercomparison Project (Tonga-MIP) (Clyne et al. 2024) and the Hunga Tonga-Hunga
129 Ha'apai Volcano Impact Model Observation Comparison (HTHH-MOC) Project (this paper).
130 The HTHH-MOC provides a foundation for a coordinated multi-model evaluation of global
131 chemistry-climate models' performance in response to the Hunga volcanic eruption. It defines a
132 set of perturbation experiments, where volcanic forcings—injected water vapor and aerosol
133 concentrations—are consistently applied across participating model members. HTHH-MOC
134 aims to assess how reliably global chemistry-climate models simulate the climate responses to
135 this unprecedented volcanic forcing. This project enhances our confidence in attributing and
136 interpreting observations following the Hunga eruption. The scientific questions related to the

137 HTHH-MOC are: How does the Hunga volcanic plumes' transport relate to or impact
138 stratospheric dynamics (such as Brewer-Dobson circulation, polar vortex and the Quasi-Biennial
139 Oscillation) and upper atmosphere? What are the chemical impacts of the Hunga eruption in the
140 stratosphere and mesosphere? What and how long is the radiative effect of the Hunga eruption?
141 Does Hunga impact the tropospheric/surface climate?
142 Therefore, the HTHH-MOC project is focused on evaluating global chemistry-climate
143 models regarding the following three science themes: (1) plume evolution, dispersion, and large-
144 scale transport; (2) impacts on stratospheric chemistry and the ozone layer; and (3) radiative
145 effect from the eruption and surface climate impacts. Besides the HTHH-MOC project, the
146 assessment also includes analysis of observations and models that are not global climate models.
147 In the following paragraph, we describe the HTHH-MOC experiment design and participating
148 models.
149
150 **2. Experiment Design**
151 There are two experiments (**Exp1** and **Exp2** detailed below) designed to fulfill the
152 scientific goals. Each experiment includes a set of simulations with different volcanic injections
153 (i.e. with and without water and/or SO2 injections), to explore the separate impacts of volcanic
154 water and aerosols during the post-eruption period: a) Control case (no eruption); b) H_2O (~150
155 Tg) & SO_2 (0.5 Tg); c) Only H_2O (~150 Tg). d) Only SO_2 (0.5 Tg). Simulations with the
156 injection of SO_2 only (d) are optional and designed for aerosol-focused models. The SO_2 and
157 water injections are prescribed based on Millan et al. (2022) and Carn et al. (2023). Note that
158 ~150 Tg of water is not the injection amount but the amount retained after the first couple of
159 days. This is because some models form ice particles that fall out of the stratosphere due to large
160 H_2O supersaturation during the initial injection (Zhu et al., 2022); these models will have to
161 inject more H_2O to counterbalance the ice formation (see **Table 6**). The only requirement is that
162 the model should have reasonable comparison to the MLS observations for water vapor as shown
163 in **Figure 1**. Aside from retaining ~150 Tg of water, the water vapor enhancement should be near
164 10 hPa to 50 hPa, and most of the water vapor should be located between 10˚N and 30˚S by
165 March 2022.
166 The first experiment (**Exp1**) is a free-running ensemble simulation covering the period
167 from 2022 to 2031. The experiment has been designed to answer questions on: 1. Understanding
168 the long-term evolution of Hunga water vapor and aerosols in free-running models; 2.
169 Quantifying Hunga effects on stratospheric temperatures, dynamics, and transport; 3.
170 Understanding the impact of dynamic changes on ozone chemistry; 4. Quantifying the net
171 radiative effects; 5. Estimating surface impacts (e.g., temperature, El Niño-Southern Oscillation,
172 monsoon precipitation, etc.). Simulations with free-running meteorology are required to properly
173 understand the impacts of the eruption on atmospheric dynamics and transport processes, and the
174 resulting impacts of those on chemical species (e.g., ozone) and surface climate. Since coupling
175 of the atmosphere with ocean and land processes is required to fully simulate many aspects of the
176 surface impacts, the use of coupled atmosphere, ocean, and land models is recommended.
177 However, since such a fully interactive set up imposes additional computing requirements, an
178 alternative model set up with fixed sea-surface temperatures (SSTs) and sea-ice is also allowed.
179 In that case, the prescribed climatological SSTs and sea-ice data are obtained by averaging SST
180 during the past decade (2012-2021), with the same data imposed in both the H_2O+SO_2 (b) and
181 control (a) simulations. It is important to note that both initial and boundary conditions in a
182 model come with uncertainties, and model processes are simplified. Therefore, model

183 simulations are influenced by the characteristics of the model itself and the background state of
184 the atmospheric system (Jones et al., 2016; Brodowsky et al., 2021). To address some of the
185 inherent uncertainties and reduce contribution of interannual variability to the forced response,
186 we use a large ensemble of simulations with slightly varied initial conditions. Note that in the
187 projection of stratospheric volcanic forcing, we only considered the Hunga eruption since 2022,
188 and no future explosive eruptions are included. For example, the 2024 Mt. Ruang eruption
189 contributed to elevated stratospheric aerosol optical depth, but it is not included.
190   Particularly, the first 5 years of qualified models output of **Exp1** are used to understand
191 climate impacts on the mesosphere and ionosphere from 2022-2027, such as gravity wave drag,
192 temperature changes, polar mesospheric clouds (PMCs), and atmospheric circulation. The
193 qualified models need to resolve the upper atmosphere with vertical resolutions higher or equal
194 to what we request in **Section 3**.
195   Since some aspects of the response, e.g., impacts on the radiative effect, may be too noisy
196 from free-running model simulations even with large ensembles, we have also designed the
197 second experiment which uses nudged temperature and meteorology to ensure that the
198 meteorology will be as close as possible to the one observed and thus isolate chemical changes
199 and their radiative effect. Experiment 2 (**Exp2**) is a two-year simulation that runs from 2022 to
200 2023 with nudged winds and/or temperature to answer questions on H_2O and aerosol evolution;
201 quantification of the net radiative effects; and impacts on mid-latitude and polar ozone
202 chemistry. **Exp2** has two distinct realizations: Experiment 2a (**Exp2a**) and Experiment 2b
203 (**Exp2b**). The models participating in **Exp2a** all have a prognostic aerosol module, but vary in
204 the complexity of their representation of aerosol microphysics (i.e., bulk, modal, or sectional).
205 Models participating in **Exp2b** use prescribed aerosol surface area density (SAD) and radiative
206 properties as input to the models (Jörimann, 2024). The prescribed aerosol properties are
207 calculated using Global Space-based Stratospheric Aerosol Climatology (GloSSAC; Thomason
208 et al., 2018; Kovilakam et al., 2020, 2023) version 2.22 aerosol data from 1979-2023. Note that
209 for the period after the Hunga eruption, GloSSAC uses the Stratospheric Aerosol and Gas
210 Experiment (SAGEIII/ISS) version 5.3 interpolated along the time axis and the Optical
211 Spectrograph and InfraRed Imager System (OSIRIS) version 7.3 to fill in any missing data
212 poleward of 60˚ N/S due to the unavailability of the Cloud-Aerosol Lidar and Infrared Pathfinder
213 Satellite Observations (CALIPSO) data since January 2022. Therefore, when conducting
214 analyses north/south of 60˚N/S it should be noted that the aerosols may be underestimated due to
215 the OSIRIS instrument retrieval biases. We ask for the models to check their initial chemical
216 fields against MLS to see if the models are qualified to evaluate their ozone chemistry. The
217 nudged runs of **Exp2** enable isolation of the chemical impact of the Hunga eruption from the
218 volcanically induced changes in dynamics by comparing the runs with and without H_2O+SO_2
219 injection. The net radiative effect anomaly due to water and sulfate aerosol can also be calculated
220 by comparing the control run (a) with the H_2O+SO_2 injection run (b).
221   **Table 1** shows the forcings and emissions data used for the HTHH-MOC experiments.
222 **Table 2** shows the settings specific to each experiment. For volcanic injection for **Exp1** and **2**,
223 we recommend the injections of H_2O and SO_2 at 4 UTC on Jan 15, 2022. All the models are
224 required to retain a similar amount of water as observed by MLS (~ 150 Tg). The models are
225 recommended to compare with the MLS evolution for validation (**Figure 1**). The goal is to retain
226 the same amount of water and similar altitude to start with, so we can analyze the water's impact
227 on the stratosphere and climate. If injecting 25-30 km cannot retain 150 Tg, models can inject

228 higher than 30 km. The SO_2 injection is required to be 0.5 Tg for all models. The injection
229 locations are not required to be co-injected with H_2O.
230   The data analysis of this project is designed to do inter-model comparisons, as well as
231 inter-experiment comparisons. For example, the comparisons between **Exp2a** and **Exp2b** can
232 help to understand how well we simulate the sulfate SAD and the importance of SAD variation
233 for stratospheric ozone chemistry. Comparing **Exp1** and **Exp2** for the same period can help
234 understand instantaneous and adjusted radiative effects. In addition, large (10-20) member
235 ensembles are requested for free-running simulations to better quantify the role of internal
236 variability in the climate response.
237
238 **Table 1. Summary of forcings and emissions data used in HTHH-MOC experiments.**

Spin-up*	5 years nudged runs
Degassing** and eruptive volcano source	Need both degassing and eruptive volcanic input for 5-year spin-up. Degassing continues during the experiment runs (e.g. 10 years for **Exp1**, 2 years for **Exp2**). recommended references: Volcanic degassing Carn et al. (2017); Eruptive volcanoes (Neely III, & Schmidt (2016) https://archive.researchdata.leeds.ac.uk/96/ or Carn et al. (2017); Assume no more explosive volcanoes after Hunga.
Surface emission	Coupled Model Intercomparison Project phase 6 (CMIP6) emissions follow SSP2-4.5 (Gidden et al., 2019), which adopts an intermediate greenhouse gas (GHG) emission: CO_2 emissions around current levels before beginning to decline by 2050.
Chemical initialization	Stratospheric chemistry fields (such as O_3, H_2O) at the beginning of 2022 should be compared with MLS observations for validation if the model participates in evaluation of the Hunga stratospheric chemistry impact.

239 * 5 years is enough to reach sulfate equilibrium in the stratosphere; water may take 7 years (each model
240 should adjust the spin-up time according to model features). ** Recommended degassing volcanic
241 emissions injected at the cone altitude, constant flux based on Carn et al. (2017). Database is updated
242 through 2022 here: https://doi.org/10.5067/MEASURES/SO2/DATA406.
243
244 **Table 2. Experiment design**

Experiment	Meteorology	period	aerosol treatment	QBO	SST	Ensemble members
Exp1_FixedSST				Internal generated (Nudge if model doesn't generate)	Fixed (climatology = mean of monthly average during the past decade (2012-2021), repeating annually) This applies to spin-up time too.	10-20
Exp1_CoupledOcean	Free run starts Feb 1. (i.e. nudge until Jan 31)	10 years 2022-2031 (first 5 years for mesospheric analysis)	model simulated aerosol or prescribed		Coupled ocean (optional) initialize with observed ocean state (see section 3 for individual model descriptions)	10-20
Exp2a	Nudged wind only and/or nudged T and wind*	2 years 2022-2023	model simulated aerosol	nudged	Observed SST	-
Exp2b	Nudged wind only and/or	2 years 2022-2023	prescribed	nudged	Observed SST	-

nudged T
and wind*

245
246

(a) H₂O 2022 Mar   (b) H₂O 2022 Jun   (c) H₂O 2022 Sep
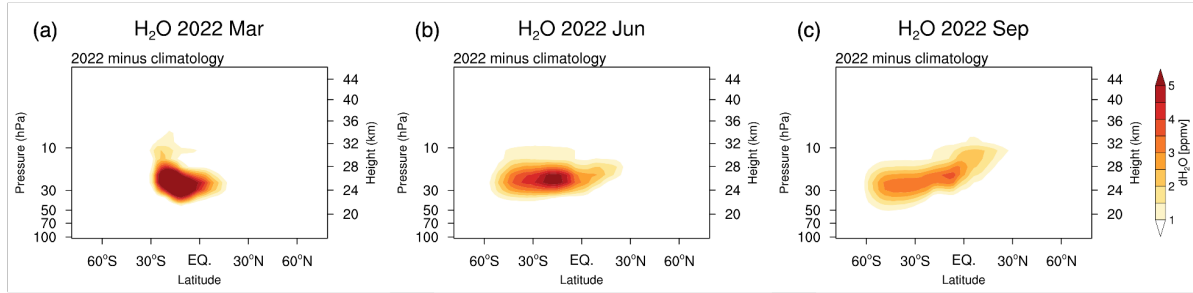
247
248 **Figure 1.** Monthly average water vapor perturbation after the Hunga eruption from MLS. Panels
249 (a-c) show the observed dispersion of the H_2O enhancement in 2022 in the months of (a) March,
250 (b) June, and (c) September.
251
252   A parallel model intercomparison project Tonga-MIP (Clyne et al., 2024) will also be
253 part of the 2025 Hunga assessment, which is designed to explore the plume evolution between 1
254 day and up to 1 or 2 months after the eruption. Tonga-MIP was initiated before the APARC
255 Hunga Activity started. It will be described in a separate paper, but we list it in this paper to
256 document the comprehensiveness of the modeling effort for the Hunga assessment. Two
257 purposes of Tonga-MIP cannot be achieved by Exp1 and 2: 1. The nudged experiment of Tonga-
258 MIP aims to intercompare the microphysics processes (i.e., cloud and aerosol physics and sulfur
259 chemistry) between different models. Therefore, all models are requested to inject 150 Tg of
260 water, but the retaining of the water varies between models, differing from Exp1 and 2, which
261 ask to retain ~150 Tg of water in the stratosphere. SO2 injection is 0.5 Tg, the same as
262 experiments in HTHHMOC. The injections are required to be injected between 25-30 km, within
263 the latitude and longitude box of 22-14°S and 182-186°E, at a constant vertical volume mixing
264 ratio for 6 hours starting at 4 UTC on January 15th. 2. The free-run experiment of Tonga-MIP
265 aims to study the radiative effect of water and SO_2 on the Hunga plume descending and
266 ascending during the first month after the eruption since the Hunga water and aerosol plumes
267 were observed to descend several kilometers during the first monthly after the eruption (Sellito et
268 al., 2022; Randel et al., 2024). Therefore, Tonga-MIP designed to nudge the atmosphere up until
269 several different dates and explore the plume descending patterns with free-run atmosphere after
270 these dates. The dates are Jan 21, Jan 26 and Jan 31. Most of the models that participate in
271 Tonga-MIP also participate in the HTHH-MOC.
272
273
274 **3. Model output**
275   The model output covers variables based on the Chemistry-Climate Modeling Initiative
276 (CCMI) output list with some additions specific to this study. The detailed list is provided in the
277 **Supplementary Excel Table**. We have requested that all models generate the same variable
278 names, units, ordering of dimensions (longitude from 0˚E to 360˚E; latitude from 90˚S to 90˚N;
279 pressure levels from 1000 hPa to 0.03 hPa or altitude from 0 meter to 85,000 meter), and file
280 name structure (e.g. 'variable_domain_modelname_experimentname.nc' or
281 'domain_modelname_experimentname.variable.nc'). The examples of Experiment_name are:
282 HTHHMOC-Exp1, HTHHMOC-Exp1and4. The example file names are:

283 Monthlymean_WACCM6MAM_HTHHMOC-Exp1-NoVolc-fixedSST.ensemble001.O3.nc or
284 O3_Dailymean_WACCM6MAM_HTHHMOC-Exp1-H2Oonly-CoupledOcean.ensemble001.nc.
285   The 3D model output is requested on both model levels (hybrid pressure or height) and
286 interpolated to CMIP6 plev39 grid (plev39: 1000, 925, 850, 700, 600, 500, 400, 300, 250, 200,
287 170, 150, 130, 115, 100, 90, 80, 70, 50, 30, 20, 15, 10, 7, 5, 3, 2, 1.5, 1 0, 0.7, 0.5, 0.4, 0.3, 0.2,
288 0.15, 0.1, 0.07, 0.05, 0.03 hPa) and for mesospheric analysis adding 0.02, 0.01, 0.007, 0.005,
289 0.003, 0.001 above the plev39 grid.
290   Monthly mean output is requested for all variables for **Exp1** with some fields (specified
291 in the Excel sheet) as daily mean. Some of the fields requested as daily means are specified,
292 either as surface fields or at reduced number of pressure levels. Daily mean output is requested
293 for all variables for **Exp2**.
294   The model output (~33 TB) **of Exp1 and Exp2** is archived at the JASMIN workspace
295 (jasmin.ac.uk). JASMIN provides large storage space and compute facilities to facilitate the data
296 archiving and post data analysis of this project. This reduces the need for data transfers and
297 allows reproducible computational workflows. Seddon et al. (2023) described the facility in
298 detail. Our next phase is to publicly release the data by transferring the data to the Centre for
299 Environmental Data Analysis (CEDA) archiving system.
300
301 **4. Model Descriptions and the Hunga Volcanic Injection Specification**
302   As part of the three-year Hunga Impact activity, this project is highly time-sensitive. We
303 designed the timeline for each experiment (**Figure 2**) to facilitate the completion of the 2025
304 Hunga Impact assessment. However, the JASMIN workspace will remain open for the uploading
305 of modeling data after the deadline denoted in **Figure 2** until 2025**.**
306   This paper only includes model descriptions for those models that submitted the output
307 following the assessment timeline. The model setup follows the protocols listed in Section 2
308 unless specified below. **Tables 3-6** provide key information on the participant models, which are
309 detailed described in the following paragraphs for each model.
310

311
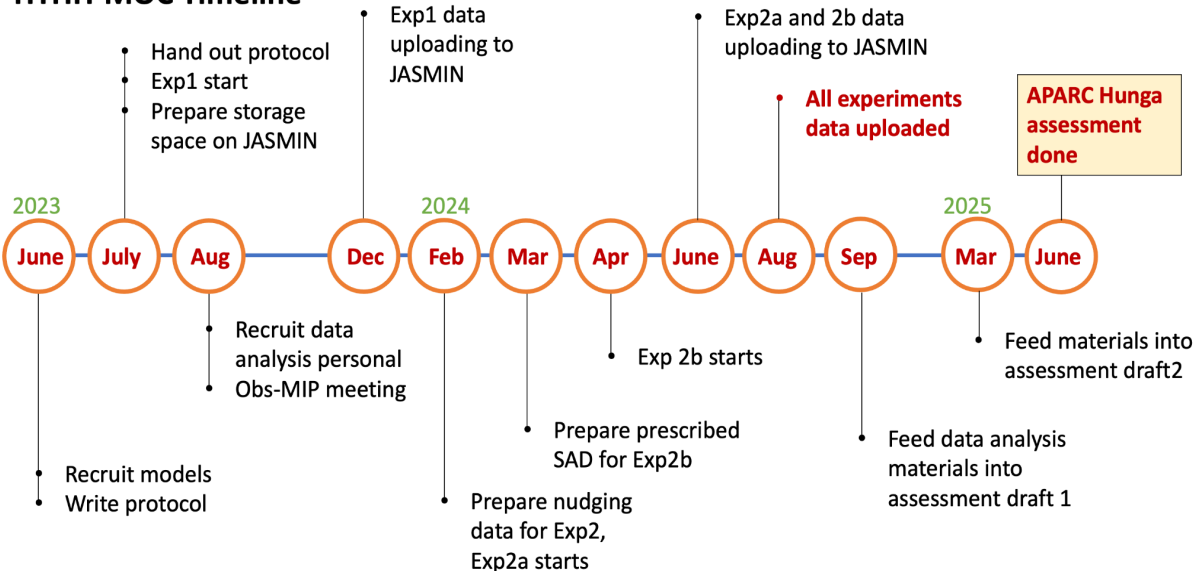
312 **Figure 2.** The timeline designed for HTHH-MOC in order to cooperate with the APARC HTHH
313 Impact assessment.
314

Table 3. Participating models and contact information for HTHH-MOC and Tonga-MIP.

Model name	Description reference paper	Institutions (**that develop the model**)	Primary contact (**who runs the model**)	Emails
CAM5/CARMA	Yu et al. (2015)	CU Boulder Jinan Univ.	Pengfei Yu Yifeng Peng	pengfei.yu@colorado.edu pengyf16@lzu.edu.cn
CCSRNIES-MIROC3.2	Akiyoshi et al. (2023), Akiyoshi et al. (2016)	NIES	Yousuke Yamashita Hideharu Akiyoshi	yamashita.yosuke@nies.go.jp hakiyosi@nies.go.jp
CMAM	Jonsson et al. (2004), Scinocca et al. (2008)	CCCma, Environment and Climate Change Canada	David Plummer	david.plummer@ec.gc.ca
EMAC MPIC	Schallock et al. (2023)	MPI-C, -M, DLR	Christoph Brühl	christoph.bruehl@mpic.de
GA4 UM-UKCA	Dhomse et al. (2020)	Univ. Leeds	Graham Mann, Sandip Dhomse	G.W.Mann@leeds.ac.uk, S.S.Dhomse@leeds.ac.uk
GEOSCCM	Nielsen et al. (2017)	NASA	Peter Colarco	peter.r.colarco@nasa.gov
GEOS/CARMA	Nielsen et al. (2017)	NASA	Parker Case	parker.a.case@nasa.gov
GSFC2D	Fleming et al. (2024)	NASA	Eric Fleming	eric.l.fleming@nasa.gov
IFS-COMPO Cy49R1	Huijnen et al. (GMD, 2016), Rémy et al. (GMD, 2022)	ECMWF and team CAMS2_35	Simon Chabrillat Samuel Rémy	Simon.chabrillat@aeronomie.be sr@hygeos.com
LMDZ6.2-LR-STRATAER/LMDZ6.2-LR-STRATAER-REPROBUS	O. Boucher et al. 2020, Marchand et al., 2012	CNRS, Sorbonne Univerité, IPSL, LATMOS, LOCEAN	Marion Marchand, Slimane Bekki, Nicolas Lebas, Lola Falletti	marion.marchand@latmos.ipsl.fr, slimane.bekki@latmos.ipsl.fr, nicolas.lebas@locean.ipsl.fr, lola.falletti@latmos.ipsl.fr
MIROC-CHASER	Sekiya et al. (2016)	JAMSTEC	Shingo Watanabe, Takashi Sekiya	wnabe@jamstec.go.jp, tsekiya@jamstec.go.jp
MIROC-ES2H	Tatebe et al. (2019), Kawamiya et al. (2020)	JAMSTEC and NIES	Shingo Watanabe, Takashi Sekiya, Tatsuya Nagashima, Kengo Sudo	wnabe@jamstec.go.jp, tsekiya@jamstec.go.jp, nagashima.tatsuya@nies.go.jp, kengo@nagoya-u.jp
SOCOLv4	Sukhodolov et al. (2021)	PMOD/WRC and ETH-Zurich	Timofei Sukhodolov	timofei.sukhodolov@pmodwrc.ch
UKESM1.1	Sellar et al. (2019, 2020), with chemistry updates from Dennison et al. (2019)	UK Met Office, UK Universities and National Centre for Atmospheric Science (NCAS)	Graham Mann, Sandip Dhomse Ben Johnson Mohit Dalvi Luke Abraham James Keeble	g.w.mann@leeds.ac.uk, s.s.dhomse@leeds.ac.uk ben.johnson@metoffice.gov.uk mohit.dalvi@metoffice.gov.uk nla27@cam.ac.uk j.keeble2@lancaster.ac.uk

| WACCM6/CARM A | Tilmes et al. (2023) | NCAR | Simone Tilmes
Cheng-Cheng Liu
Yunqian Zhu
Margot Clyne (Tonga-MIP) | tilmes@ucar.edu
chengcheng.liu@lasp.colorado.edu
yunqian.zhu@noaa.gov
margot.clyne@colorado.edu |
| WACCM6/MAM | Mills et al. (2016) | NCAR | Xinyue Wang
Simone Tilmes
Jun Zhang
Wandi Yu
Zhihong Zhuo
Ewa Bednarz
Margot Clyne (Tonga-MIP) | xinyuew@colorado.edu
tilmes@ucar.edu
jzhan166@ucar.edu
yu44@llnl.gov
zhuo.zhihong@uqam.ca
ewa.bednarz@noaa.gov
margot.clyne@colorado.edu |

316

317 **Table 4. Participating models in HTHH-MOC and Tonga-MIP.**

Model names	Exp1_FixedSST	Exp1_Coupled Ocean	Exp2a	Exp2b	Tonga-MIP (clyne et al. 2024)
CAM5/CARMA			X		
CCSRNIES-MIROC3.2				X	
CMAM	X (H2O-only) (*)				
EMAC MPIC			X		
GA4 UM-UKCA					X
GEOSCCM	X		X		X
GEOS/CARMA			X		
GSFC2D	X (*)			X	
IFS-COMPO			X		
LMDZ6.2-LR-STRATAER			X		X
LMDZ6.2-LR-STRATAER-REPROBUS			X		X
MIROC-CHASER	X		X		
MIROC-ES2H					X
SOCOLv4					X
UKESM1.1			X		X
WACCM6/CARMA			X		X
WACCM6/MAM	X(*)	X(*)	X		X

318 * The models that are qualified to analyze the mesospheric components are marked with *
319 symbol.

320

321 **Table 5. Model resolutions and schemes used for HTHH-MOC experiments**

Model names	Horizontal resolution	nlevels	Model Top	Vertical resolution in the stratosphere	Aerosol scheme	Specified dynamic source	QBO for models participating free run	Chemistry package (tropospheric chemistry included?)
CAM5/CARMA	~2 deg	56	45 km	1-4 km	CARMA sectional (20 bins)	GEOS5	-	MOZART (yes)
CCSRNIES-MIROC3.2	T42	34	0.01 hPa	1-3 km	None	MERRA-2	-	full strat; no tropo
CMAM	T47	80	0.0006 hPa	0.8 - 2.5 km	None	ERA5	nudged	stratospheric + methane-NOx in troposphere
EMAC MPIC	T63	90	0.01 hPa	0.5km in LS	GMXE, modal	ERA-5	-	MECCA, simplified troposphere
GEOSCCM	c90 (~1 deg)	72	0.01 hPa	~1 km	GOCART (Bulk)	MERRA-2/GEOS-FP	Internal generated	GMI (yes)
GEOS/CARMA	c90 (~1 deg)	72	0.01 hPa	~1 km	CARMA (sectional 24 bins)	MERRA-2/GEOS-FP	-	GMI (yes)
GSFC2D	4°	76	.002 hPa (~92 km)	1km	Prescribed only	MERRA-2	Internal generated	full strat; partial trop
IFS-COMPO	T_L511 (~40km)	137	0.01 hPa	0.5-1.5 km	Bulk	ERA5	-	BASCOE (strato) + CB05 (tropo)
LMDZ6.2-LR-STRATAER	2.5° × 1.3°	79	80km	1-5 km	S3A(sectional 36 bins)	ERA5	-	No
LMDZ6.2-LR-STRATAER-REPROBUS	2.5° × 1.3°	79	80km	1-5 km	S3A(sectional 36 bins)	ERA5	-	REPROBUS
MIROC-CHASER	T85	81	0.004 hPa	0.7-1.2 km	MAM3	MERRA-2	Internal generated	troposphere-stratosphere chemistry
UKESM1.1	N96	85	80km	0.6-0.7km in LS	GLOMAP-mode	ERA-5	Internal generated	CheST strat-trop chemistry
WACCM6/CARMA	~1 deg	70	140 km	1-2 km	Sectional (20 bins)	MERRA-2	-	MOZART (yes)
WACCM6/MAM	~1 deg	70	140 km	1-2 km	MAM4	MERRA-2	Internal generated	MOZART (yes)

322
323
324 **Table 6. Hunga volcanic injection profile for HTHH-MOC experiments**

Model names	Data and duration	H_2O amount	H_2O altitude	H_2O location/area	SO_2 amount	SO_2 altitude	SO_2 location/area

				(left after a week)			
CAM5/CARMA	Jan 15, 6 hrs	150 Tg (~135 Tg)	25-35 km	22-14°S, 182-186°E	0.5 Tg	20-28 km	22-14°S, 182-186°E
CCSRNIES-MIROC3.2	Jan 15, instantly	150 Tg (~150 Tg)	12.0-27.6 hPa	181.4–187.0°E, 14.0–22.3°S	-	-	-
CMAM	Feb 20, 5 days	150 Tg (~150 Tg)	near 25.5 km	zonally average	-	-	-
EMAC MPIC	Jan 16, 12hrs	136 Tg (~130 Tg)	Gaussian centered at 21.5hPa	23-19°S, 177-173°W	0.4 Tg based on obs.	23-27 km based on obs.	30°S-5°N, 90-120°W (330°)
GEOSCCM	Jan 15, 6 hrs	750 Tg (~150 Tg)	25-30 km	22-14°S, 182-186°E	0.5 Tg	25-30 km	22-14°S, 182-186°E
GEOS/CARMA	Jan 15, 6 hrs	750 Tg (~150 Tg)	25-30 km	22-14°S, 182-186°E	0.5 Tg	25-30 km	22-14°S, 182-186°E
GSFC2D	use MLS H_2O profile until March 1	~150 Tg (~150 Tg)	-	zonally average	-	-	-
IFS-COMPO	Jan 15, 3 hrs	190 Tg (~150 Tg)	25-30 km	400 km by 200 km centered 20˚S and 175˚W	0.5 Tg	25-30 km	400 km by 200 km centered 20˚S and 175˚W
LMDZ6.2-LR-STRATAER	Jan 15, 1 day	150 Tg (~150 Tg)	Gaussian centered at 27.5 km and standard deviation of 2.5 km	22°-14°S, 182-186°E	0.5 Tg	Gaussian centered at 27.5 km and standard deviation of 2.5 km	22-14°S, 182-186°E
LMDZ6.2-LR-STRATAER-REPROBUS	Jan 15, 1 day	150 Tg (~150 Tg)	Gaussian centered at 27.5 km and standard deviation of 2.5 km	22-14°S, 182-186°E	0.5 Tg	Gaussian centered at 27.5 km and standard deviation of 2.5 km	22-14°S, 182-186°E
MIROC-CHASER	Jan 15 4 UTC, 6 hours	186 Tg (~150 Tg)	25-30 km	22-14°S, 182-186°E	0.5 Tg	25-30 km	22-14°S, 182-186°E
UKESM1.1	Jan 15, 6 hours	150 Tg	25-30km	22-14ºS 182-186°E	0.5Tg	25-30km	22-14°S, 182-186°E
WACCM6/CARMA	Jan 15, 6 hours	150 Tg (~135 Tg)	25-35 km	22-14°S, 182-186°E	0.5 Tg	20-28 km	22-14°S, 182-186°E
WACCM6/MAM	Jan 15, 6 hours	150 Tg	25-35km	22-6°S,182.5-202.5°E	0.5 Tg	26.5-36 km	22-6°S,182.5-202.5°E

(~150 Tg)		

4.1 CAM5/CARMA

The atmospheric component of the Community Atmosphere Model version 5 (CAM5) (Lamarque et al., 2012) is the atmospheric component of the Community Earth System Model, version 1 (CESM1.2.2, Hurrell et al., 2013), with a top at around 45 km. CAM5 has a horizontal resolution of 1.9° latitude × 2.5° longitude, utilizing the finite volume dynamical core (Lin & Rood, 1996). The model has 56 vertical levels, with a vertical resolution ~1 km in the upper troposphere and lower stratosphere. The modeled winds and temperatures were nudged to the 3-hour Goddard Earth Observing System 5 (GEOS-5) reanalysis data set (Molod et al., 2015) every time step (30 min) by 1% (i.e., a 50 h Newtonian relaxation time scale). The aerosol is interactively simulated using a sectional aerosol microphysics model, the Community Aerosol and Radiation Model for Atmospheres (CARMA, Yu et al., 2015). The model uses the Model for Ozone and Related Chemical Tracers (MOZART) chemistry that is used for both tropospheric (Emmons et al., 2010) and stratospheric chemistry (English et al., 2011; Mills et al., 2016). The volcanic emissions from continuously degassing volcanoes uses the emission inventory RCP8.5 and FINNv1.5. No volcanic eruptions except the Hunga 2022 eruption are included.

The initial volcanic injection altitude and area are determined by validating the water and aerosol transportation in months shown in **Figure 1** following the tests in Zhu et al. (2022), Wang et al. (2023) and Zhang et al. (2024). In these simulations, the H_2O is injected at 25 to 35 km altitude and SO_2 injected at 20 to 28 km altitude. The injection latitude ranges from 22°S to 14°S, and longitude ranges from 182°E to 186°E (Zhu et al., 2022). The initial injection of H_2O is 150 Tg, with ~ 135 Tg left after the first week following the eruption.

4.2 CCSRNIES-MIROC3.2

The Center for Climate System Research/National Institute for Environmental Studies - Model for Interdisciplinary Research on Climate version 3.2 Chemistry Climate Model (CCSRNIES-MIROC3.2 CCM) (Akiyoshi et al. 2023) was developed based on versions 3.2 of the MIROC atmospheric general circulation model (AGCM), incorporating a stratospheric chemistry module that was developed at National Institute for Environmental Studies (NIES) and the University of Tokyo. The model has a horizontal resolution of T42 (2.8° latitude × 2.8° longitude) and 34 vertical levels, with a vertical resolution ~1 km in the lower stratosphere/upper troposphere and ~3 km in the upper stratosphere and mesosphere. The top level is located at 0.01 hPa (approximately 80 km).

The chemistry in the CCSRNIES-MIROC3.2 CCM is a stratospheric chemistry module including 42 photolysis reactions, 142 gas-phase chemical reactions and 13 heterogeneous reactions for multiple aerosol types (Akiyoshi et al., 2023). Tropospheric chemistry is not included, but the stratospheric chemistry scheme is used for both the troposphere and mesosphere.

In the CCSRNIES-MIROC3.2 CCM, only **Exp2b** can be performed. The atmospheric temperature and horizontal winds are nudged toward Modern-Era Retrospective analysis for Research and Applications Version 2 (MERRA-2) reanalysis (Gelaro et al., 2017) with a 1-day relaxation using instant values at 6-hour interval (Akiyoshi et al., 2016). The HadISST data is used during the simulation.

The CCSRNIES-MIROC3.2 CCM does not have any microphysics scheme for volcanic aerosols. The surface area and spectral optical parameters of extinction, single scattering albedo,

and asymmetric factor for Hunga aerosols were prescribed in the model from the GloSSAC version 2.22 aerosol data (Jörimann 2024). H_2O was injected instantly on 15 January 2022 at the 12 grids of the model in the region 181.4°E–187.0°E in longitude, 14.0°S–22.3°S in latitude, and 12.0 hPa–27.6 hPa in pressure level. A uniform number density of 1.709×10^{15} molecules/cm^3 H_2O was injected in each of the 12 grids which amounts to ~150 Tg.

4.3 CMAM

The Canadian Middle Atmosphere Model (CMAM) is based on a vertically extended version of CanAM3.1, the third generation Canadian Atmospheric Model (Scinocca et al., 2008). Compared to the standard configuration of CanAM3.1, for CMAM the model top was raised to 0.0006 hPa (approximately 95 km) and the parameterization of non-orographic gravity wave drag (Scinocca, 2003) and additional radiative processes important in the middle atmosphere (Fomichev et al., 2004) have been included. The gas-phase chemistry includes a comprehensive description of the inorganic Ox, NOx, HOx, ClOx and BrOx families, along with CH_4, N_2O, six chlorine containing halocarbons, CH_3Br and, to account for an additional 5 ppt of bromine from short-lived source gases, CH_2Br_2 and $CHBr_3$ (Jonsson et al., 2004). A prognostic description of, and associated heterogeneous chemical reactions on water ice PSCs (PSC Type II) and liquid ternary solution (PSC Type Ib) particles is included, although gravitational settling (dehydration/denitrification) is not calculated and species return to the gas phase when conditions no longer support the existence of PSC particles.

The simulations for the HTHH-MOC simulations were performed at T47 spectral resolution (approximately 3.8° resolution on the linear transform grid used for the model physics), with 80 vertical levels giving a vertical resolution of approximately 0.8 km at 100 hPa, increasing to 2.3 km above 0.1 hPa. The CMAM does not internally generate a QBO, so the zonal winds in the equatorial region were nudged towards a dataset based on observed variations up to December 2023, constructed using the method of Naujokat (1986) and extended into the future by repeating a historical period that is congruent with the observed QBO in late 2023. Water vapor from the Hunga eruption was added as a zonally average perturbation to the model water over five days from 00 UTC on February 20, 2022. The spatial distribution of the anomaly was designed to reproduce the water vapor anomaly observed in mid-February by the The Atmospheric Chemistry Experiment - Fourier Transform Spectrometer (ACE-FTS) (Bernath et al., 2005) satellite (Patrick Sheese, personal communication), with a maximum value of 13.3 ppm at 17°S and 25.5 km and producing an anomaly of ~150 Tg H_2O in the stratosphere.

4.4 EMAC MPIC

The chemistry-climate model EMAC (ECHAM5/MESSy Atmospheric Chemistry) consists of the European Centre Hamburg general circulation model (ECHAM5) and the Modular Earth Submodel System (MESSy) (e.g., Jöckel et al., 2010). Here we use the version of Schallock et al. (2023) in horizontal resolution T63 (1.87°x 1.87°) with 90 levels between the surface and 0.01 hPa.

Vorticity, divergence, and temperatures between boundary layer and 100 hPa are nudged to the ERA5 reanalysis of ECMWF (Hersbach et al., 2020), as well as surface pressure. SSTs and sea ice cover are prescribed by ERA5 data. The model can generate an internal QBO but for comparison with observations it was slightly nudged to the Singapore data compiled by Free University of Berlin and Karlsruhe Institute of Technology.

415   The model contains gas-phase and heterogeneous chemistry on PSCs and interactive
416 aerosols. Surface mixing ratios of chlorine- and bromine-containing halocarbons and other long-
417 lived gases are nudged to Advanced Global Atmospheric Gases Experiment (AGAGE)
418 observations. The microphysical modal aerosol module contains four soluble and three insoluble
419 modes for sulfate, nitrate, dust, organic and black carbon, and aerosol water (Pringle et al.,
420 2010). The instantaneous radiative effect by tropospheric and stratospheric aerosols can be
421 calculated online by multiple calls of the radiation module. Volcanoes injecting material into the
422 stratosphere are considered as in Schallock et al. (2023) using the perturbations of stratospheric
423 SO_2 observed by the Michelson Interferometer for Passive Atmospheric Sounding (MIPAS) and
424 aerosol extinction observed by OSIRIS. This method, based typically on data of a 10-day period,
425 distributes the injected SO_2 over a larger volume than typical point source approaches using the
426 same integrated mass (see also Kohl et al., 2024). For Hunga this method has the disadvantage
427 that H_2O and SO_2 are not co-injected since H_2O is injected in 12 hours in a slab consisting of
428 four horizontal boxes and a Gaussian vertical distribution centered at 21.5 hPa. For **Exp2a** we
429 continue the 30-year transient simulation presented in Schallock et al. (2023) with and without
430 Hunga Tonga. The simulated H_2O-perturbation is consistent with **Figure 1**. The SO_2 injection is
431 derived based on the extinction from the OSIRIS observation averaged over about 10 days
432 (**Figure 3**) (Bruehl et al., 2023).
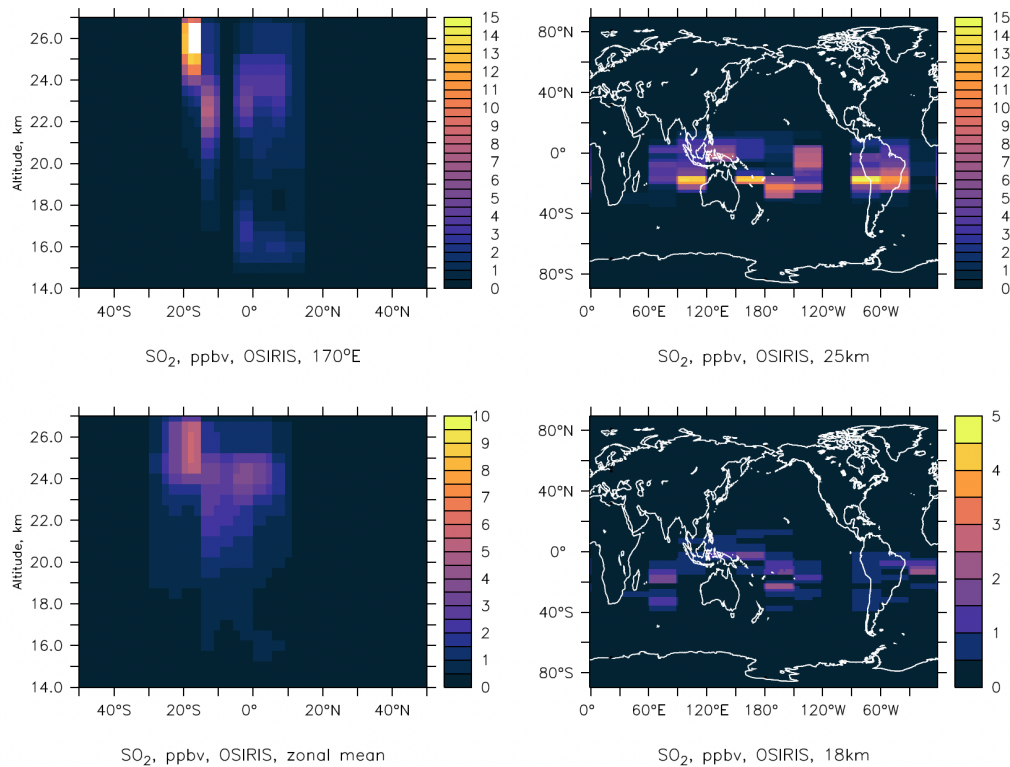
433
434 **Figure 3.** The SO_2 injection used in EMAC MPIC model is based on the Hunga SO_2
435 perturbation derived from extinction observed by OSIRIS averaged over about 10 days, i.e.,
436 including several snapshots of the westward moving plume. For conversion from extinction to
437 volume mixing ratio Eqn. 1 of Schallock et al (2023) is applied with f=3 because of data gaps.
438 5day-averaged gridded OSIRIS data averaged from January 24 0h to February 3 0h were used.
439 Note that the colorbars are not the same in each panel.
440

441
4.5 GEOSCCM

The NASA Goddard Earth Observing System Chemistry-Climate Model (GEOSCCM) is based on the GEOS Earth system model (Reinecker et al. 2008, Molod et al. 2015). For the HTHH-MOC experiments the model is run on a cubed-sphere horizontal grid at a C90 resolution (~100 km) with 72 vertical hybrid-sigma levels from the surface to 0.01 hPa (~80 km). Dynamics are solved using the finite-volume dynamical core (Putman and Lin, 2007). Deep and shallow convection are parameterized using the Grell-Freitas (2014) and Park-Bretherton (2009) schemes, respectively, and moist physics is from Bacmeister et al. (2006). The turbulence parameterization is based on the non-local scheme of Lock et al. (2000). Shortwave and longwave radiative fluxes are computed in 30 bands using the Rapid Radiative Transfer Model for GCMs (RRTMG, Iacono et al. 2008).

Stratospheric and tropospheric chemistry are from the Global Modeling Initiative (GMI) mechanism (Duncan et al., 2007; Strahan et al., 2007; Nielsen et al., 2017), updated here to include reactions for sulfur species. The GMI mechanism in GEOSCCM has been extensively evaluated for its stratospheric ozone-related photochemistry and transport in various model intercomparisons, including Stratosphere-troposphere Processes and their Role in Climate (SPARC) Chemistry Climate Model Validation (CCMVal), CCMVal-2, and the CCMI (SPARC-CCMVal, 2010; Eyring et al., 2010, 2013; Morgenstern et al., 2017). Aerosol species are simulated by the Goddard Chemistry, Aerosol, Radiation, and Transport, second generation (GOCART-2G), module (Collow et al. 2024), which includes a sectional approach for dust (five bins), sea salt (five bins), and nitrate (three bins), and a bulk approach for sulfate (dimethyl sulfide, SO_2, methanesulfonic acid, and SO_4^{2-}) aerosol and carbonaceous species (hydrophobic and hydrophilic modes of "white" and "brown" organics and black carbon).

For the GEOSCCM simulations performed with the GOCART-2G module we use the nominal GOCART-2G sulfate mechanism, updated here to use the online hydroxyl (OH) radical, nitrate (NO_3) radical, and hydrogen peroxide (H_2O_2) from the GMI mechanism instead of climatological fields provided from offline files (Collow et al., 2024). While not a full coupling to the GMI sulfur cycle it nevertheless allows the GOCART-2G sulfate mechanism to have the impact of the Hunga water vapor perturbation on the oxidants. A second "instance" of the GOCART-2G sulfate mechanism is run that is specifically for the volcanic SO_2 and resultant sulfate from the Hunga eruption. This allows us to track the eruptive volcanic aerosol separately from the nominal sulfate instance that sees mainly tropospheric sources. We assign this volcanic instance optical properties consistent with SAGE retrievals of the sulfate aerosol properties, using an effective radius of 0.4 microns. We find that 750 Tg of H_2O is needed in the initial injection to provide a residual ~150 Tg of water in the stratosphere after a week. All other injection parameters follow the protocol. The model spinup was performed by "replaying" to the MERRA-2 meteorology (Gelaro et al. 2017), and is used throughout the **Exp2a** results. A MERRA-2 2012-2021 climatology of SST and sea ice fractions are used based on Reynolds et al. (2002).

4.6 GEOS/CARMA

A second configuration of the GEOSCCM, coupled to the sectional aerosol microphysics package CARMA, also simulated the eruption (GEOS/CARMA). This configuration is the same as above except for the aerosol package and its coupling to the GMI chemistry mechanism. For this version of GEOSCCM, we use the configuration of CARMA described in Case et al. (2023).

This configuration uses 24 size bins, spread logarithmically in volume between 0.25nm and 6.7μm in radius and simulates the nucleation, condensational growth, evaporation, coagulation, and settling of sulfate aerosols in these simulations following the mechanism of English et al. (2013). For these simulations, CARMA is fully coupled to the GMI sulfur cycle by the production (i.e., oxidation of SO_2, evaporation of sulfate aerosols) and loss (i.e., nucleation and condensation of sulfate aerosols) of sulfuric acid (H_2SO_4) vapor. Optical properties for the CARMA aerosols are calculated based on the interactively calculated aerosol size distribution. The same injection parameters for GEOSCCM described above are used by this configuration. This model configuration contributed to **Exp2a** and "replayed" to MERRA-2 meteorology as above.

4.7 GSFC2D

The NASA/Goddard Space Flight Center two-dimensional (2D) chemistry-climate model (GSFC2D) has a domain extending from the surface to ~92 km (0.002 hPa). The model has 76 levels, with 1 km vertical resolution from the surface to the lower mesosphere (60 km) and 2 km resolution above (60-92 km). The horizontal resolution is 4° latitude, and the model uses a 2D (latitude-altitude) finite volume dynamical core (Lin & Rood, 1996) for advective transport. The model has detailed stratospheric chemistry and reduced tropospheric chemistry, with a diurnal cycle computed for all constituents each day (Fleming et al., 2024). The model uses prescribed zonal mean surface temperature as a function of latitude and season based on a multi-year average of MERRA-2 data (Gelaro et al., 2017). Zonal mean latent heating, tropospheric water vapor, and cloud radiative properties as a function of latitude, altitude, and season are also prescribed (Fleming et al., 2020).

For the free-running simulations, the model planetary wave parameterization (Bacmeister et al., 1995; Fleming et al., 2024) uses lower boundary conditions (750 hPa, ~2 km) of geopotential height amplitude and phase for zonal wave numbers 1–4. These are derived as a function of latitude and season using: 1) a 30-year average (1991–2020) of MERRA-2 data for the standard yearly-repeating climatological-dynamics simulations ("Clim-NoQBO"); and 2) individual years of MERRA-2 data (1980-2020) randomly rearranged in time to generate interannual variations in stratospheric dynamics ("ensemble1", "ensemble2",…"ensemble10"). For the inter-annually varying dynamics simulations, the model includes an internally generated QBO (Fleming et al., 2024).

For experiments that include the Hunga volcanic aerosols, the simulations go through the end of 2023, using prescribed aerosol properties for 2022-2023 from both the GloSSAC data set and derived from the OMPS-LP data (Taha et al., 2021, 2022). For experiments that include the Hunga H_2O injection, Aura/MLS observations are used to derive a daily zonal mean Hunga water vapor anomaly in latitude-altitude, which is added to the baseline H_2O (no volcano) through the end of February 2022. This combined water vapor field is then fully model computed starting 1 March 2022 through the end of 2031.

For **Exp2b**, the model zonal mean temperature and transport fields are computed from the MERRA-2 reanalysis data. These are input into the model and used as prescribed fields (no nudging is done).
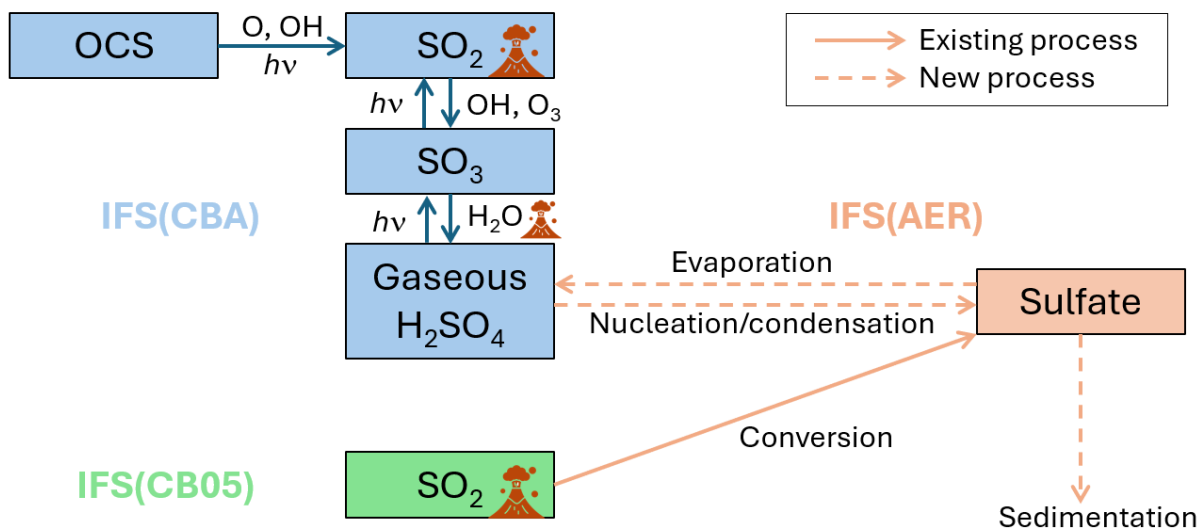
4.8 IFS-COMPO

The Copernicus Atmosphere Monitoring Service (CAMS) provides daily global analysis and 5-day forecasts of atmospheric composition (aerosols, trace gases, and GHGs) (Peuch et al.

2022). CAMS is coordinated by the European Centre for Medium Range Weather Forecasts (ECMWF) and uses, for its global component, the Integrated Forecasting System (IFS), with extensions to represent aerosols, trace, and GHGs, being called "IFS-COMPO" (also previously known as "C-IFS", Flemming et al. 2015). IFS-COMPO is composed of IFS(AER) for aerosols, as described in Remy et al. (2022) while the atmospheric chemistry is based on the chemistry module as described in Williams et al. (2022) for the troposphere (IFS-CB05) and Huijnen et al. (2016) for the stratosphere (IFS-CBA). The stratospheric chemistry module of IFS-COMPO is derived from the Belgian Assimilation System for Chemical ObErvations (BASCOE, Errera et al 2019). IFS-COMPO stratospheric chemistry is used since the operational implementation of cycle 48R1 on June 27, 2023 (Eskes et al., 2024).

The aerosol component of IFS-COMPO is a bulk aerosol scheme for all species except sea salt aerosol and desert dust, for which a sectional approach is preferred, with three bins for each of these two species. Since the implementation of operational cycle 48R1 in June 2023, the prognostic species are sea salt, desert dust, organic matter (OM), black carbon (BC), sulfate, nitrate, ammonium, and secondary organic aerosols (SOA).

For **Exp2a**, cycle 49R1 IFS-COMPO has been used, which will become operational for CAMS production in November 2024, at a resolution of TL511 (~40 km grid cell) over 137 model levels from surface to 0.01 hPa. Cycle 49R1 IFS-COMPO integrates a number of updates of tropospheric and stratospheric aerosols and chemistry. The most relevant aspect for this work concerns the representation of stratospheric aerosols, which has been revisited with the implementation of a coupling to the stratospheric chemistry through a simplified stratospheric sulfur cycle including nucleation/condensation and evaporation processes, as shown in **Figure 4**. Direct injection of water vapor into the stratosphere is expected to enhance the nucleation and condensation of sulfate through the reaction with SO_3 and production of gas-phase H_2SO_4.

The volcanic injection takes place between 3 and 6 UTC on January 15, 2022, with a uniform vertical distribution between 25 and 30 km of altitude, over a rectangular region of 400 km (latitude) x 200 km (longitude) centered on the coordinates of the Hunga volcano. The injected quantities are 0.5 Tg SO_2 and 190 Tg H_2O.

Figure 4. Architecture of the stratospheric extension of IFS(AER) and its coupling with IFS(CBA) and IFS(CB05), with existing and new processes implemented in cycle 49R1 of IFS-COMPO. $h\nu$

565 represents photolysis and the volcano symbols represent direct injections by volcanic eruptions.
566 Sedimentation is indicated as a new process because it has been revisited.
567
568
569 **4.9 LMDZ6.2-LR-STRATAER and LMDZ6.2-LR-STRATAER-REPROBUS**
570   The Institut Pierre-Simon Laplace Climate Modelling Centre (IPSL CMC, see
571 https://cmc.ipsl.fr) has set up a new version of its climate model in the runup of CMIP6. Further
572 description of the IPSL-CM6A-LR climate model can be found in Boucher et al. (2020) and in
573 Lurton et al. (2020). New development of the model is now ongoing to prepare the IPSLCM7
574 version.
575   The IPSLCM7 climate model is using the general circulation model named LMDZ for
576 *Laboratoire de Météorologie Dynamique-Zoom* (Hourdin et al., 2006). The LMDZ version used
577 for this study is based on a regular horizontal grid with 144 points regularly spaced in longitude
578 and 142 in latitude, corresponding to a resolution of 2.5° × 1.3°. The model has 79 vertical layers
579 and extends up to 80 km, which makes it a "high-top" model. The model shows a self-generated
580 quasi-biennial oscillation (QBO) whose period has been tuned to the observed one for the
581 present-day climate (Boucher et al., 2020).
582   The aerosol is interactively simulated in the STRATAER module using a sectional
583 scheme with 36 size bins. STRATAER is an improved version of the Sectional Stratospheric
584 Sulfate Aerosol (S3A) module (Kleinschmitt et al., 2017). It now takes into account the
585 photolytic conversion of H_2SO_4 into SO_2 in the upper stratosphere (Mills et al., 2005). The size-
586 dependent composition of H_2SO_4/H_2O aerosols is now computed iteratively to ensure that the
587 surface tension, density, and composition are consistent in the calculation of the Kelvin effect.
588 The surface tension, density, H_2SO_4 vapor pressure, and nucleation rates are calculated based on
589 Vehkamäki et al. (2002). The version of the LMDZ6.2-LR-STRATAER atmospheric model used
590 in the HTHH Impact project accounts for the stratospheric H_2O source from methane oxidation.
591 The chemistry is simulated using the REPROBUS (*REactive Processes Ruling the Ozone
592 BUdget in the Stratosphere*) chemistry module that includes 55 chemical species and a
593 comprehensive description of the stratospheric chemistry (Marchand et al., 2012, Lefèvre et al.,
594 1994, Lefèvre et al., 1998).
595   For **Exp2a**, the H_2O and SO_2 is injected at 27.5 km altitude using a Gaussian distribution
596 and standard deviation of 2.5 km. The injection latitude ranges from 22°S to 14°S, and longitude
597 ranges from 182°E to 186°E. The injections of H_2O and SO_2 are 150 Tg and 0.5 Tg, respectively.
598 The SSTs are taken from the IPSL climate coupled simulation run under the CMIP6 Tier 1
599 SSP2-4.5 scenario (Neil et al., 2016).
600
601 **4.10 MIROC-CHASER**
602   The Model for Interdisciplinary Research On Climate - CHemical Atmospheric general
603 circulation model for Study of atmospheric Environment and Radiative forcing (MIROC-
604 CHASER) version 6 (Sekiya et al. 2016) is a chemistry climate model, with a top at around 0.004
605 hPa. The present version of MIROC-CHASER is built on MIROC6 (Tatebe et al. 2019) and has a
606 spectral horizontal resolution of T85 (1.4° latitude × 1.4° longitude). The model has 81 vertical
607 levels, with a vertical resolution 0.7 km in the lower stratosphere, ~1.2 km in the upper stratosphere,
608 and ~3 km in the lower mesosphere. In the free-running simulations, the model generates
609 QBO internally. The ensemble members have different initial conditions (January 1, 2022), which
610 are generated using slightly different nudging relaxation time during the spin-up. The aerosols are

interactively simulated using a three-mode modal aerosol module (Seikiya et al. 2016). The chemistry uses comprehensive troposphere-stratosphere chemistry (Watanabe et al. 2011). The volcanic emission from continuously degassing volcanoes uses the emission inventory of Fioletov et al. (2022). For the explosive volcanic eruptions during the spin-up time, explosive volcanic emissions follow Carn (2022).

For **Exp1** fixed SST simulations, the model uses the observed SST from 10-year climatological mean from 2012 to 2021 using the montly-1deg CMIP6 AMIP SST (Gates et al., 1999).

For **Exp2a**, the atmospheric temperature and winds are nudged to MERRA-2 reanalysis with a 12-hour relaxation using 3-hour meteorology. The observed SST uses the NOAA 1/4° Daily Optimum Interpolation Sea Surface Temperature (OISST) from 2022 to 2023 (Huang et al. 2020).

The initial volcanic injection altitude and area are not tuned but follow the experimental protocol. For **Exp1** and **Exp2a**, the H_2O and SO_2 are injected at 25 to 30 km altitude. The injection latitude ranges from 22°S to 14°S, and longitude ranges from 182°E to 186°E. The initial injection of H_2O is 186 Tg, with ~150 Tg left after the first week following the eruption. The large initial H_2O injection is necessary to keep 150 Tg in the stratosphere as requested by the experimental protocol, because a large amount of ice clouds generates and falls to the troposphere soon after the eruption.

4.11 UKESM1.1

The United Kingdom Earth System Model (UKESM, Sellar et al., 2019, 2020) is the successor to the HadGEM2-ES model (Collins et al., 2011), jointly developed by the UK Met Office and the Natural Environment Research Council (NERC) to deliver simulations to the Coupled Model Intercomparison Project Phase 6 (CMIP6; Eyring et al., 2016). For HTHH-MOC, we run the updated UKESM1.1 system (Mulcahy et al., 2023) which consists of the physical climate model HadGEM3-GC3.1 (Kuhlbrodt et al., 2018; Williams et al., 2018), and has improved tropospheric aerosol processes and aerosol radiative forcings (Mulcahy et al., 2018; 2020). The GC3.1 system comprises the GA7.1 global atmosphere model configuration (Walters et al., 2019), which uses the ENDGAME dynamics system (Wood et al., 2014), at a resolution of 1.875° longitude by 1.25° latitude with 85 levels extending to 85 km. Specifically the simulations apply the UKESM1.1-AMIP academic community release job (at v12.1 of the Unified Model), as supported by the UK National Centre for Atmospheric Science.

The interactive atmospheric chemistry module UKCA (UK Chemistry and Aerosols) has a number of chemistry configurations; with UKESM1.0 for CMIP6 applying the combined stratosphere and troposphere chemistry (CheST) option (Archibald et al., 2020), essentially a combination of the stratosphere chemistry (Morgenstern et al., 2009) and tropospheric chemistry (O'Connor et al., 2014) UKCA schemes. The UKCA aerosol scheme is the GLOMAP-mode aerosol microphysics module (Mann et al., 2010; 2012; Bellouin et al., 2013), with UKESM1.0 including the initial set of adaptations to GLOMAP for simulating stratospheric aerosol (Dhomse et al., 2014). For all UKESM1.0 integrations for CMIP6, the system was applied with evaporation of sulphate aerosol de-activated, stratospheric aerosol properties enacted from the CMIP6 prescribed zonal mean data set (Luo, 2017), but for the integrations here we have applied the system for interactive aerosol across the troposphere and stratosphere, enacting a Hunga emission of volcanic SO_2 following the 0.5Tg@25-30km Tonga-MIP protocols (see **Table 6**).

For the improved UKESM1.1 version applied here, the other most relevant development, compared to UKESM1.0 used for CMIP6, is the interactive atmospheric chemistry module UKCA

657   (UK Chemistry and Aerosols) has the updates to heterogeneous chemistry added by Dennison et
658   al. (2019), to represent more realistically reactions occurring on the surfaces of polar stratospheric
659   clouds and sulfate aerosol, with modified uptake coefficients of the five existing reactions and the
660   addition of a further eight reactions involving bromine species.   For these simulations, we have
661   added to UKESM for the first time the equilibrium liquid PSC scheme of Carslaw et al. (1995), an
662   interim implementation here coupling the 5 existing heterogeneous reactions chlorine activation
663   then occurring on both solid and now also liquid ternary-aerosol PSCs.
664   For **Exp2**, UKESM1.1 is run in specified dynamics configuration (Telford et al., 2008,
665   2009), the atmospheric temperature and winds nudged to ERA5 every 6 hours, the Newton
666   relaxation applied for levels 12 to 80 of 85 (between 1 km and 60 km) Sea-surface temperatures
667   and sea-ice are prescribed from the Reynolds v2.1 datasets, both during the 2017 to 2022 spin-up
668   period, and the 2-year experiment 2 period to December 2023.   Monthly varying anthropogenic
669   atmospheric chemistry and aerosol emissions were set following the CMIP6 SSP2-4.5 datasets.
670
671

672   **4.12 WACCM6/MAM4**
673   The Whole Atmosphere Community Climate Model version 6 (WACCM6; Gettelman et
674   al. 2019) is the high-top version of the atmospheric component of the Community Earth System
675   Model, version 2 (CESM2), with a top at around 140 km. WACCM6 has a horizontal resolution
676   of 0.9° latitude × 1.25° longitude, utilizing the finite volume dynamical core (Lin & Rood,
677   1996). The model has 70 vertical levels, with a vertical resolution ~1 km in the lower
678   stratosphere, ~1.75 km in the upper stratosphere, and ~3.5 km in the upper mesosphere and lower
679   thermosphere (Garcia et al., 2017). In the free-running simulations, the model generates QBO
680   internally (Mills et al., 2017; Gettelman et al. 2019). The ensemble members differ in the last
681   date of nudging (from January 27 to February 5, 2022). The aerosol is interactively simulated
682   using a four-mode modal aerosol module (MAM4; Liu et al., 2012, 2016; Mills et al., 2016), in
683   which we used the Vehkamäki nucleation scheme (Vehkamäki et al., 2002). The chemistry uses
684   comprehensive troposphere-stratosphere-mesosphere-lower-thermosphere (TSMLT) chemistry
685   (Gettelman et al. 2019). The volcanic emissions from continuously degassing volcanoes use the
686   emission inventory of Andres and Kasgnoc (1998). For the explosive volcanic eruptions during
687   the spin-up time, explosive volcanic emissions follow Mills et al. (2016) and Neely III and
688   Schmidt (2016) with updates until 2022.
689   For **Exp1_CoupledOcean** simulations, the ocean and sea-ice are initialized on January
690   3, 2022 with output from a standalone ocean model forced by atmospheric state fields and fluxes
691   from the Japanese 55-year Reanalysis (Tsujino et al., 2018). To accurately simulate the early
692   plume structure and evolution, the winds and temperatures in WACCM are nudged toward the
693   Analysis for Research and Applications, MERRA-2 meteorological data (Gelaro et al., 2017)
694   throughout January 2022. After February 1, 2022, the model is free-running to capture fully-
695   coupled variability. For the fixed SST simulation, the model uses the 10-year climatology SST
696   from 2012 to 2021. The SST data is OISSTv2, which is a NOAA High-resolution (0.25x0.25)
697   Blended Analysis of Daily SST and Ice (Banzon et al., 2022).

698   For **Exp2**, the atmospheric temperature and winds are nudged to MERRA-2 reanalysis
699   with a 12-hour relaxation using 3-hour meteorology (Davis et al., 2022). The observed SST uses
700   10-year climatological mean from 2012 to 2021.
701   The initial volcanic injection altitude and area are the same as described for section 4.1
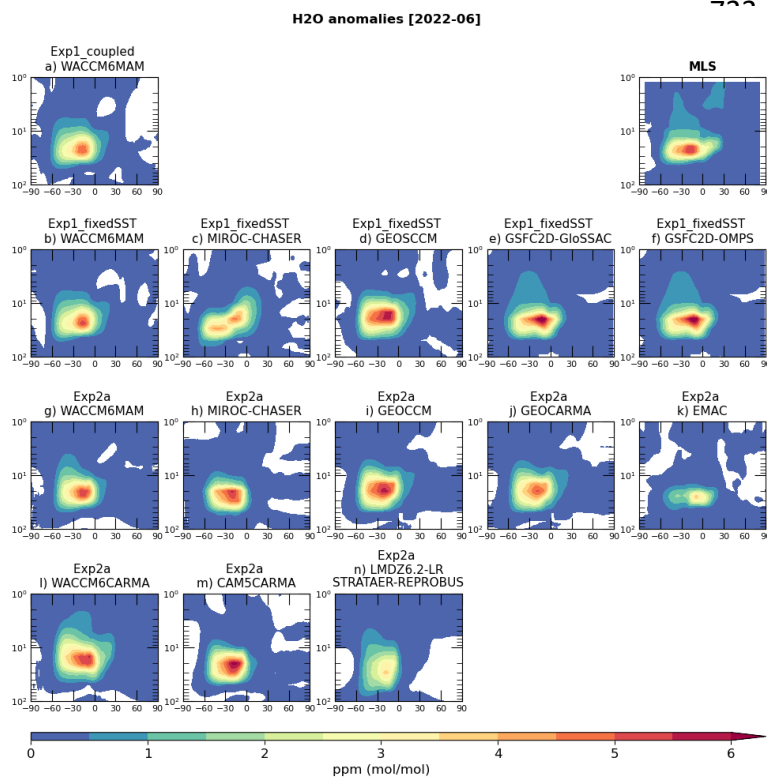702   CAM5/CARMA.
703
704   **4.13 WACCM6/CARMA**
705   WACCM6/CARMA only performed **Exp2** and used a configuration similar to
706   WACCM6/MAM4 with the same horizontal and vertical resolution, SSTs, and meteorological
707   nudging. Differences compared to WACCM6/MAM4 are the chemistry and aerosol
708   configuration used. WACCM6/CARMA used the middle atmosphere chemistry with limited
709   chemistry in the troposphere and comprehensive chemistry in the stratosphere, mesosphere and
710   lower thermosphere (Davis et al., 2022). Furthermore, we use the Community Aerosol and
711   Radiation Model for Atmospheres (CARMA, Tilmes et al. 2023, based on Yu et al., 2015 with
712   some updates) as the aerosol module, in which we used the Vehkamäki nucleation scheme
713   (Vehkamäki et al., 2002). CARMA defines 20 mass bins and tracks the dry mass of the particles
714   and assumes particle water is in equilibrium with the environmental water vapor. The
715   approximate radius ranges from 0.2 nm to 1.3 μm in radius for the pure sulfate group that sulfate
716   homogeneous nucleation occurs in, and ranges from 0.05 to 8.7 μm in the mixed group that
717   tracks all major tropospheric aerosol types (i.e. black carbon, organic carbon, sea salt, dust,
718   sulfate).
719   The initial volcanic injection altitude and area are determined by validating the water and
720   aerosol transportation in the first six months against MLS and OMPS observations. In these
721   simulations, the H_2O is injected to 25 to 35 km altitude following Zhu et al. (2022), while the SO_2
722   is injected 82% of the total mass to 26.5-28 km and 18% to 28-36 km altitude. The injection latitude
723   ranges from 22°S to 6°S, and longitude ranges from 182.5°E to 202.5°E.
724

5. Preliminary results

The models' performances will be evaluated focusing on the following aspects: the stratospheric aerosol optical depth will be compared with GloSSAC and other satellite instruments individually such as OMPS-LP, SAGEIII-ISS, and OSIRIS; the aerosol effective radius will be compared with balloon observations (Asher et al., 2024), SAGEIII-ISS retrieved size distribution and AeroNet retrieved particle radius; the water vapor lifetime, ozone and its related chemicals (such as HCl, HNO3, CLO) will be compared with MLS observations; the temperature anomaly will be compared with MLS detrended temperature field (Randel et al., 2024). All the evaluations will be conducted before looking into the climate impact of this eruption, such as radiative impact and tropospheric responses. This work will be described in a follow up manuscript.

As this manuscript is written, we are still completing the model output inspection and validation phase. So, we can only provide preliminary results from some models. **Figure 5** shows the preliminary results from Exp1 and Exp2 in June 2022 compared with the MLS v5 water vapor anomaly. The model results shown here generally agree with MLS anomaly regarding the vertical (10-50 hPa) and horizontal distribution (60˚S to 20˚N), and the anomaly peaking at ~ 6 ppmv for most of the models. This consistency of water vapor anomaly six months after the eruption helps us have confidence in these models on the analysis of climate and chemistry impacts, and will be evaluated in detail in the follow up studies.

Figure 5. the zonal average H_2O anomaly in June 2022 from MLS, Exp1_fixedSST, Exp1_CoupledOcean and Exp2a. The simulated anomaly is using H_2O+SO_2 run minus the control run. And the MLS uses the 2022 data minus the climatology.

6. Summary

A multi-model observation comparison project is designed to evaluate the impact of the 2022 Hunga eruption. Two experiments are designed to cover various research interests for this eruption, including sulfate and water plume dispersion and transport, dynamical and chemical responses in the stratosphere, and climate impact. The project will not only benefit the Hunga Impact assessment, but also benchmark the model performance on simulating stratospheric explosive volcanic eruption events and stratospheric water vapor injections. These events have a

24

770 potentially large impact on the Earth system, especially on the stratospheric ozone layer and
771 radiative balance.
772
773

774 **Code/Data availability**
775

783

784 **Author Contributions:**
785 Y.Z. Concept design, Project Administration, Experiment design, data archive, WACCM models
786 setup;
787 E.A. provides NOAA balloon aerosol and water vapor observations for experiments
788 E.B. and S.T. and J.Z. Experiment design, conducts experiments using WACCM6MAM;
789 A.B. Experiment design, Data archive;
790 A.J. Experiment 2b prescribed fields preparation;
791 M.K. provides GloSSAC data for Exp 2b;
792 Takashi S. and S.W.: S.W. conducted all MIROC-CHASER experiments, data post-processing,
793 data archive under supervision of Takashi S., who developed the aerosol microphysics scheme of
794 the model.
795 X.W. and W.Y. Conducts experiment using WACCM6MAM;
796 Z.Z. Conducts experiment using WACCM6MAM, WACCM6MAM data post-processing, data
797 archive;
798 N.L. and S.B.: Conducts experiment using IPSL7-STRATAER, data post-processing and archive
799 M.M. and L.F.: Conducts experiment using IPSL7-STRATAER-REPROBUS, data post-
800 processing and archive
801 S.R. and S.C. Conducts experiments using IFS-COMPO
802 M.C. Experiment design, Tonga-MIP lead;
803 F.F.Ø., G.K., O.M. contributed to experiment design
804 C.B. Conducts experiment using EMAC
805 I.Q., V.A., R.U. and A.K. Model output inspection and evaluation
806 E.F. Conducts experiments using GSFC2D, data post-processing, and data archive.
807 D.P. Contributed to experiment design and conducted experiments using CMAM and data post-
808 processing
809 P.R.C., L.D.O., Q.L., M.M., and S.S. Contributed to experiment design and conducted
810 experiments with the NASA GEOS CCM
811 P.C. and P.R.C. Contributed to experiment design and conducted experiments with the NASA
812 GEOS CARMA model
813 H.A. and Y.Y. Conducts experiment using CCSRNIES-MIROC3.2, data post-processing and
814 archive
815 D.V. contributed to experiment design and assisted E.B. with variables request
816 W.R. and P.N. concept design

817 G.M. concept design and in charge of JASMIN data archiving
818 P.Y. and Y.P. conduct experiments using CAM5CARMA and data post-processing
819 S.T. and C.-C. L. conduct experiments using WACCM6CARMA and data post-processing
820
821 **Competing interests**
822 We declare at least one of the co-authors is on the editorial board of GMD.
823

References:

Akiyoshi, H., M. Kadowaki, Y. Yamashita, T. Nagatomo (2023), Dependence of column ozone on future ODSs and GHGs in the variability of 500-ensemble members. Sci. Rep. 13, 320(1–12). https://doi.org/10.1038/s41598-023-27635-y

Akiyoshi, H., T. Nakamura, T. Miyasaka, M. Shiotani, and M. Suzuki (2016), A nudged chemistry-climate model simulation of chemical constituent distribution at northern high-latitude stratosphere observed by SMILES and MLS during the 2009/2010 stratospheric sudden warming, J. Geophys. Res. Atmos., 121, 1361-1380, doi:10.1002/2015JD023334

Andres, R. J., and A. D. Kasgnoc (1998), A time-averaged inventory of subaerial volcanic sulfur emissions, J. Geophys. Res., 103(D19), 25,251–25,261, doi:10.1029/98JD02091.

Archibald, A. T., O'Connor, F. M., Abraham, N. L., Archer-Nicholls, S., Chipperfield, M. et al.: Description and evaluation of the UKCA stratosphere–troposphere chemistry scheme (StratTrop vn 1.0) implemented in UKESM1, *Geosci. Model Dev., 13, 1223–1266,* https://doi.org/10.5194/gmd-13-1223-2020, 2020

Bacmeister, J. T., Schoeberl, M. R., Summers, M. E., Rosenfield, J. E., & Zhu, X. (1995). Descent of long-lived trace gases in the winter polar vortex. Journal of Geophysical Research, 100(D6), 11669–11684. https://doi.org/10.1029/94jd02958

Bacmeister, J. T., Suarez, M. J., & Robertson, F. R. (2006). Rain reevaporation, boundary layer–convection interactions, and Pacific rainfall patterns in an AGCM. *Journal of the Atmospheric Sciences*, *63*(12), 3383-3403.

Banzon, Viva &, Reynolds, Richard & National Center for Atmospheric Research Staff (Eds). Last modified 2022-09-09 "The Climate Data Guide: SST data: NOAA High-resolution (0.25x0.25) Blended Analysis of Daily SST and Ice, OISSTv2." Retrieved from https://climatedataguide.ucar.edu/climate-data/sst-data-noaa-high-resolution-025x025-blended-analysis-daily-sst-and-ice-oisstv2 on 2025-02-04.

Bellouin, N., Mann, G. W., Woodhouse, M. T., Johnson, C. E., Carslaw, K. S. and Dalvi, M. Impact of the modal aerosol scheme GLOMAP-mode on aerosol forcing in the Hadley Centre Global Environmental Model, Atmos. Chem. Phys., 13, 3027–3044, https://doi.org/10.5194/acp-13-3027-2013, 2013.

Bernath, P. F., McElroy, C. T., Abrams, M. C., Boone, C. D., Butler, M., Camy-Peyret, C., Carleer, M., Clerbaux, C., Coheur, P.-F., Colin, R., DeCola, P., DeMazière, M., Drummond, J. R., Dufour, D., Evans, W. F. J., Fast, H., Fussen, D., Gilbert, K., Jennings, D. E., Llewellyn, E. J., Lowe, R. P., Mahieu, E., McConnell, J. C., McHugh, M., McLeod, S. D., Michaud, R., Midwinter, C., Nassar, R., Nichitiu, F., Nowlan, C., Rinsland, C. P., Rochon, Y. J., Rowlands, N., Semeniuk, K., Simon, P., Skelton, R., Sloan, J. J., Soucy, M.-A., Strong, K., Tremblay, P., Turnbull, D., Walker, K. A., Walkty, I., Wardle, D. A.,

Wehrle, V., Zander, R., and Zou, J., Atmospheric Chemistry Experiment (ACE): Mission overview, Geophysical Research Letters, 32, https://doi.org/10.1029/2005GL022386, 2005.

Boucher O., Servonnat, J., Albright, A. L., Aumont, O., Balkanski, Y., Bastrikov, V., et al. (2020). Presentation and evaluation of the IPSL-CM6A-LR climate model. Journal of Advances in Modeling Earth Systems, 12, e2019MS002010. https://doi.org/10.1029/2019MS002010.

Bretherton, C. S., & Park, S. (2009). A new moist turbulence parameterization in the Community Atmosphere Model. *Journal of Climate*, *22*(12), 3422-3448.

Brodowsky, C., Sukhodolov, T., Feinberg, A., Höpfner, M., Peter, T., Stenke, A., & Rozanov, E. (2021). Modeling the sulfate aerosol evolution after recent moderate volcanic activity, 2008–2012. *Journal of Geophysical Research: Atmospheres*, 126, e2021JD035472. https://doi.org/10.1029/2021JD035472

Bruehl, C., Lelieveld, J., Schallock, J., & Rieger, L. A. (2023, December). Chemistry Climate Model Studies on the Effect of the Hunga Tonga Eruption on stratospheric Ozone in mid and high Latitudes in 2022. In *AGU Fall Meeting Abstracts* (Vol. 2023, No. 2235, pp. A21B-2235).

Carn, S., Clarisse, L., and Prata, A.: Multi-decadal satellite measurements of global volcanic degassing, J. Volcanol. Geoth. Res., 311, 99–134, https://doi.org/10.1016/j.jvolgeores.2016.01.002, 2016.

Carn, S., Fioletov, V., McLinden, C. et al. A decade of global volcanic SO_2 emissions measured from space. Sci Rep 7, 44095 (2017). https://doi.org/10.1038/srep44095

Carn, S. (2022), Multi-Satellite Volcanic Sulfur Dioxide L4 Long-Term Global Database V4, Greenbelt, MD, USA, Goddard Earth Science Data and Information Services Center (GES DISC), Accessed: [6/9/2024], 10.5067/MEASURES/SO2/DATA405

Case, P., Colarco, P. R., Toon, B., Aquila, V., & Keller, C. A. (2023). Interactive stratospheric aerosol microphysics-chemistry simulations of the 1991 Pinatubo volcanic aerosols with newly coupled sectional aerosol and stratosphere-troposphere chemistry modules in the NASA GEOS Chemistry-Climate Model (CCM). *Journal of Advances in Modeling Earth Systems*, *15*(8), e2022MS003147.

Clyne, M., Lamarque, J.-F., Mills, M. J., Khodri, M., Ball, W., Bekki, S., Dhomse, S. S., Lebas, N., Mann, G., Marshall, L., Niemeier, U., Poulain, V., Robock, A., Rozanov, E., Schmidt, A., Stenke, A., Sukhodolov, T., Timmreck, C., Toohey, M., Tummon, F., Zanchettin, D., Zhu, Y., and Toon, O. B.: Model physics and chemistry causing intermodel disagreement within the VolMIP-Tambora Interactive Stratospheric Aerosol ensemble, Atmos. Chem. Phys., 21, 3317–3343, https://doi.org/10.5194/acp-21-3317-2021 , 2021.

Clyne, M.: Modeling the Role of Volcanoes in the Climate System – Chapter 4: Tonga-MIP, Ph.D. dissertation, University of Colorado at Boulder, ProQuest Dissertations & Theses, 31487034, 153 pp., 2024.

Collins, W. J., Bellouin, N., Doutriaux-Boucher, M., Gedney, N., Halloran, P., Hinton, T., et al. Development and evaluation of an Earth-System model-HadGEM2. Geoscientific Model Development. https://doi.org/10.5194/gmd-4-1051-2011, 2011.

A. Collow, P. Colarco, A. da Silva, V. Buchard, H. Bian, M. Chin, S. Das, R. Govindaraju, D. Kim, V. Aquila: Benchmarking GOCART-2G in the Goddard Earth Observing System (GEOS), Geoscientific Model Development, 17, 1443–1468, doi: 10.5194/gmd-17-1443-2024 (2024).

Davis, N. A., Callaghan, P., Simpson, I. R., and Tilmes, S.: Specified dynamics scheme impacts on wave-mean flow dynamics, convection, and tracer transport in CESM2 (WACCM6), Atmos.Chem. Phys., 22, 197–214, https://doi.org/10.5194/acp-22-197-2022, 2022.

Dennison, F., Keeble, J., Morgenstern, O., Zeng, G., Abraham, N. L. and Yang, X.: Improvements to stratospheric chemistry scheme in the UM-UKCA (v10.7) model: solar cycle and heterogeneous reactions, Geosci. Mod. Dev., 12, 1227–1239, 2019.

Dhomse, S. S., Emmerson, K. M., Mann, G. W., Bellouin, N., Carslaw, K. S., Chipperfield, M. P. et al.: Aerosol microphysics simulations of the Mt. Pinatubo eruption with the UM-UKCA composition-climate model, Atmos. Chen. Phys., 14, 11221–11246, 2014

Dhomse, S. S., Mann, G. W., Antuña Marrero, J. C., Shallcross, S. E., Chipperfield, M. P., Carslaw, K. S., Marshall, L., Abraham, N. L., and Johnson, C. E.: Evaluating the simulated radiative forcings, aerosol properties, and stratospheric warmings from the 1963 Mt Agung, 1982 El Chichón, and 1991 Mt Pinatubo volcanic aerosol clouds, Atmos. Chem. Phys., 20, 13627–13654, https://doi.org/10.5194/acp-20-13627-2020, 2020.

Duncan, B. N., Logan, J. A., Bey, I., Megretskaia, I. A., Yantosca, R. M., Novelli, P. C., ... & Rinsland, C. P. (2007). Global budget of CO, 1988–1997: Source estimates and validation with a global model. *Journal of Geophysical Research: Atmospheres*, *112*(D22).

Gates, W. L., Boyle, J. S., Covey, C., Dease, C. G., Doutriaux, C. M., Drach, R. S., Fiorino, M., Gleckler, P. J., Hnilo, J. J., Marlais, S. M., Phillips, T. J., Potter, G. L., Santer, B. D., Sperber, K. R., Taylor, K. E., and Williams, D. N.: An Overview of the Results of the Atmospheric Model Intercomparison Project (AMIP I), B. Am. Meteorol. Soc., 80, 29–55, 1999.

English, J. M., Toon, O. B., Mills, M. J., and Yu, F.: Microphysical simulations of new particle formation in the upper troposphere and lower stratosphere, Atmos. Chem. Phys., 11, 9303-9322, 10.5194/acp-11-9303-2011, 2011.

English, J. M., Toon, O. B., & Mills, M. J. (2013). Microphysical simulations of large volcanic eruptions: Pinatubo and Toba. *Journal of Geophysical Research: Atmospheres*, *118*(4), 1880-1895.

Errera, Q., Chabrillat, S., Christophe, Y., Debosscher, J., Hubert, D., Lahoz, W., Santee, M. L., Shiotani, M., Skachko, S., von Clarmann, T., and Walker, K.: Technical note: Reanalysis of Aura MLS chemical observations, Atmos. Chem. Phys., 19, 13647–13679, https://doi.org/10.5194/acp-19-13647-2019, 2019.

Eskes, H., Tsikerdekis, A., Ades, M., Alexe, M., Benedictow, A. C., Bennouna, Y., Blake, L., Bouarar, I., Chabrillat, S., Engelen, R., Errera, Q., Flemming, J., Garrigues, S., Griesfeller, J., Huijnen, V., Ilić, L., Inness, A., Kapsomenakis, J., Kipling, Z., Langerock, B., Mortier, A., Parrington, M., Pison, I., Pitkänen, M., Remy, S., Richter, A., Schoenhardt, A., Schulz, M., Thouret, V., Warneke, T., Zerefos, C., and Peuch, V.-H.: Technical note: Evaluation of the Copernicus Atmosphere Monitoring Service Cy48R1 upgrade of June 2023, Atmos. Chem. Phys., 24, 9475–9514, https://doi.org/10.5194/acp-24-9475-2024, 2024.

Eyring, V., Cionni, I., Bodeker, G. E., Charlton-Perez, A. J., Kinnison, D. E., Scinocca, J. F., ... & Yamashita, Y. (2010). Multi-model assessment of stratospheric ozone return dates and ozone recovery in CCMVal-2 models. *Atmospheric Chemistry and Physics*, *10*(19), 9451-9472. https://doi.org/10.5194/acp-10-9451-2010

Eyring, V., Bony, S., Meehl, G. A., Senior, C A., Stevens, B. et al., Overview of the Coupled Model Intercomparison Project Phase 6 (CMIP6) experimental design and organization, Geosci. Model Dev., 9, 1937–1958, https://doi.org/10.5194/gmd-9-1937-2016, 2016

Fioletov, V., McLinden, C. A., Griffin, D., Abboud, I., Krotkov, N., Leonard, P. J. T., Li, C., Joiner, J., Theys, N., and Carn, S. (2022), Multi-Satellite Air Quality Sulfur Dioxide (SO2) Database Long-Term L4 Global V2, Edited by Peter Leonard, Greenbelt, MD, USA, Goddard Earth Science Data and Information Services Center (GES DISC), Accessed: [6/9/2024], 10.5067/MEASURES/SO2/DATA406

Fleming, E. L., Newman, P. A., Liang, Q., & Daniel, J. S. (2020). The impact of continuing CFC-11 emissions on stratospheric ozone. Journal of Geophysical Research: Atmospheres, 125(3), e2019JD031849. https://doi.org/10.1029/2019jd031849

Fleming, E. L., Newman, P. A., Liang, Q., & Oman, L. D. (2024). Stratospheric temperature and ozone impacts of the Hunga Tonga-Hunga Ha'apai water vapor injection. Journal of Geophysical Research: Atmospheres, 129(1), e2023JD039298. https://doi.org/10.1029/2023JD039298

Flemming, J., Huijnen, V., Arteta, J., Bechtold, P., Beljaars, A., Blechschmidt, A.-M., Diamantakis, M., Engelen, R. J., Gaudel, A., Inness, A., Jones, L., Josse, B., Katragkou, E., Marecal, V., Peuch, V.-H., Richter, A., Schultz, M. G., Stein, O., and Tsikerdekis, A.: Tropospheric chemistry in the Integrated Forecasting System of ECMWF, Geosci. Model Dev., 8, 975–1003, 2015.685 https://doi.org/10.5194/gmd-8-975-2015

Fomichev, V. I., Fu, C., de Grandpre, J., Beagley, S. R., Ogibalov, V. P., and McConnell, J. C.: Model thermal response to minor radiative energy sources and sinks in the middle atmosphere, J. Geophys. Res., 109, D19107, doi:10.1029/2004JD004892, 2004.

Gelaro, R., and Coauthors, 2017: The Modern-Era Retrospective Analysis for Research and Applications, Version 2 (MERRA-2). J. Climate, 30, 5419–5454, https://doi.org/10.1175/JCLI-D-16-0758.1.

Gettelman, A., Mills, M. J., Kinnison, D. E., Garcia, R. R., Smith, A. K., Marsh, D. R., Tilmes, S., Vitt, F., Bardeen, C. G., McInerney, J., Liu, H.-L., Solomon, S. C., Polvani, L. M., Emmons, L. K., Lamarque, J.-F., Richter, J. H., Glanville, A. S., Bacmeister, J. T., Phillips,

A. S., Neale, R. B., Simpson, I. R., DuVivier, A. K., Hodzic, A., and Randel, W. J.: The Whole Atmosphere Community Climate Model Version6 (WACCM6), J. Geophys. Res.-Atmos., 124, 12380–12403, https://doi.org/10.1029/2019JD030943, 2019.

Gidden, M. J., Riahi, K., Smith, S. J., Fujimori, S., Luderer, G., Kriegler, E., ... & Takahashi, K. (2019). Global emissions pathways under different socioeconomic scenarios for use in CMIP6: a dataset of harmonized emissions trajectories through the end of the century. Geoscientific model development, 12(4), 1443-1475. https://doi.org/10.5194/gmd-12-1443-2019

Grell, G. A., & Freitas, S. R. (2014). A scale and aerosol aware stochastic convective parameterization for weather and air quality modeling. *Atmospheric Chemistry and Physics*, *14*(10), 5233-5250. https://doi.org/10.5194/acp-14-5233-2014

Hersbach H, Bell B, Berrisford P, et al. (2020). The ERA5 global reanalysis. *Quarterly Journal of the Royal Meteorological Society*, 146: 1999–2049. https://doi.org/10.1002/qj.3803

Hourdin, F., Musat, I., Bony, S., Braconnot, P., Codron, F., Dufresne, J.-L., Fairhead, L., Filiberti, M.-A., Friedlingstein, P., Grandpeix, J.-Y., Krinner, G., Levan, P., Li, Z.-X., and Lott, F.. The LMDZ4 general circulation model : climate performance and sensitivity to parametrized physics with emphasis on tropical convection. Climate Dynamics, 27 :787–813, 2006.

Huang, B., C. Liu, V. Banzon, E. Freeman, G. Graham, B. Hankins, T. Smith, and H.-M. Zhang, 2020: Improvements of the Daily Optimum Interpolation Sea Surface Temperature (DOISST) Version 2.1, Journal of Climate, 34, 2923-2939. doi: 10.1175/JCLI-D-20-0166.1

Huijnen, V., Flemming, J., Chabrillat, S., Errera, Q., Christophe, Y., Blechschmidt, A.-M., Richter, A., and Eskes, H.: C-IFS-CB05-BASCOE: stratospheric chemistry in the Integrated Forecasting System of ECMWF, Geoscientific Model Development, 9, 3071–3091, 2016.705

Hurrell, J. W., et al. (2013), The community Earth system model: A framework for collaborative research, Bull. Am. Meteorol. Soc., doi:10.1175/ BAMS-D-12-00121.

Iacono, M. J., Delamere, J. S., Mlawer, E. J., Shephard, M. W., Clough, S. A., & Collins, W. D. (2008). Radiative forcing by long-lived greenhouse gases: Calculations with the AER radiative transfer models. *Journal of Geophysical Research: Atmospheres*, *113*(D13).

Jöckel, P., Kerkweg, A., Pozzer, A., Sander, R., Tost, H., Riede, H., Baumgaertner, A., Gromov, S., and Kern, B.: Development cycle 2 of the Modular Earth Submodel System (MESSy2), Geosci. Model Dev., 3, 717–752, 2010.

Jones, A. C., J. M. Haywood, A. Jones, V. Aquila. Sensitivity of volcanic aerosol dispersion to meteorological conditions: a Pinatubo case study, J. Geophys. Res., 121(12), 6892-6908, doi: 10.1002/2016JD025001, 2016.

Jonsson, A. I., de Grandpré, J., Fomichev, V. I., McConnell, J. C., and Beagley, S. R., Doubled CO_2-induced cooling in the middle atmosphere: Photochemical analysis of the ozone radiative feedback, J. Geophys. Res., 109, D24103, doi:10.1029/2004JD005093, 2004.

Kawamiya, M., Hajima, T., Tachiiri, K. et al. Two decades of Earth system modeling with an emphasis on Model for Interdisciplinary Research on Climate (MIROC). Prog Earth Planet Sci 7, 64. https://doi.org/10.1186/s40645-020-00369-5, (2020).

Kleinschmitt, C., Boucher, O., Bekki, S., Lott, F., and Platt, U.: The Sectional Stratospheric Sulfate Aerosol module (S3A-v1) within the LMDZ general circulation model: description and evaluation against stratospheric aerosol observations, Geosci. Model Dev., 10, 3359–3378, 2017, https://doi.org/10.5194/gmd-10-3359-2017.

Kohl, M., C. Brühl, J. Schallock, H. Tost, P. Jöckel, A. Jost, S. Beirle, M. Höpfner, and A. Pozzer (2024). New submodel for emissions from Explosive Volcanic ERuptions (EVER v1.1) within the Modular Earth Submodel System (MESSy, version 2.55.1), https://doi.org/10.5194/egusphere-2024-2200.

Kovilakam, M., Thomason, L. W., Ernest, N., Rieger, L., Bourassa, A., and Millán, L. (2020), The Global Space-based Stratospheric Aerosol Climatology (version 2.0): 1979–2018, Earth Syst. Sci. Data, 12, 2607–2634, https://doi.org/10.5194/essd-12-2607-2020.

Kovilakam, M., Thomason, L., and Knepp, T.: SAGE III/ISS aerosol/cloud categorization and its impact on GloSSAC, Atmos. Meas. Tech., 16, 2709–2731, https://doi.org/10.5194/amt-16-2709-2023, 2023.

Kuhlbrodt, T., Jones, C. G., Sellar, A., Storkey, D., Blockley, E., Stringer, M., et al. (2018). The Low–Resolution Version of HadGEM3 GC3.1: Development and Evaluation for Global Climate. Journal of Advances in Modeling Earth Systems, 10, 2865–2888. https://doi.org/10.1029/2018MS001370, 2018.

Lamarque, J.-F., et al. (2012), CAM-chem: Description and evaluation of interactive atmospheric chemistry in the Community Earth System Model, Geosci. Model Dev., 5(2), 369–411, doi:10.5194/gmd-5-369-2012.

Lefèvre, F., Brasseur, G. P., Folkins, I., Smith, A. K., and Simon, P.: Chemistry of the 1991–1992 stratospheric winter: Three-dimensional model simulations, J. Geophys. Res.-Atmos., 99, 8183–8195, https://doi.org/10.1029/93JD03476, 1994.

Lefèvre, F., Figarol, F., Carslaw, K. S., and Peter, T.: The 1997 Arctic Ozone depletion quantified from three-dimensional model simulations, Geophys. Res. Lett., 25, 2425–2428, https://doi.org/10.1029/98GL51812, 1998.

Jörimann, A., 2024. REMAP-GloSSAC-2023 [dataset]. ETH Zürich, url: http://hdl.handle.net/20.500.11850/713396. doi: 10.3929/ethz-b-000713396.

Li, C., Peng, Y., Asher, E., Baron, A. A., Todt, M., Thornberry, T. D., et al. (2024). Microphysical simulation of the 2022 Hunga volcano eruption using a sectional aerosol model. Geophysical Research Letters, 51, e2024GL108522. https://doi.org/10.1029/2024GL108522

Lin, S. J., & Rood, R. B. (1996). Multidimensional flux-form semi-Lagrangian transport schemes. Monthly weather review, 124(9), 2046-2070. https://doi.org/10.1175/1520-0493(1996)124%3C2046:MFFSLT%3E2.0.CO;2

Liu, X., Easter, R. C., Ghan, S. J., Zaveri, R., Rasch, P., Shi, X., Lamarque, J.-F., Gettelman, A., Morrison, H., Vitt, F., Conley, A., Park, S., Neale, R., Hannay, C., Ekman, A. M. L., Hess, P., Mahowald, N., Collins,W., Iacono, M. J., Bretherton, C. S., Flanner, M. G., and Mitchell, D.: Toward a minimal representation of aerosols in climate models: description and evaluation in the Community Atmosphere Model CAM5, Geosci. Model Dev., 5, 709–739, https://doi.org/10.5194/gmd-5-709-2012, 2012.

Liu, X., Ma, P.-L., Wang, H., Tilmes, S., Singh, B., Easter, R. C., Ghan, S. J., and Rasch, P. J.: Description and evaluation of a new four-mode version of the Modal Aerosol Module (MAM4) within version 5.3 of the Community Atmosphere Model, Geosci. Model Dev., 9, 505–522, https://doi.org/10.5194/gmd-9-505-2016, 2016.

Lock, A. P., Brown, A. R., Bush, M. R., Martin, G. M., & Smith, R. N. B. (2000). A new boundary layer mixing scheme. Part I: Scheme description and single-column model tests. *Monthly weather review*, *128*(9), 3187-3199.

Lurton, T., Balkanski, Y., Bastrikov, V., Bekki, S., Bopp, L., Braconnot, P., et al. (2020). Implementation of the CMIP6 forcing data in the IPSL-CM6A-LR model. Journal of Advances in Modeling Earth Systems, 12, e2019MS001940. https://doi.org/10.1029/2019MS001940

Mann, G. W., Carslaw, K. S., Spracklen, D. V., Ridley, D. A., Manktelow, P. T., Chipperfield, M. P., Pickering, S. J. and Johnson, C. E.: Description and evaluation of GLOMAP-mode: a modal global aerosol microphysics model for the UKCA composition-climate model Geosci. Mod. Dev., 3, 519-551, https://doi.org/10.5194/gmd-3-519-2010, 2010.

Mann, G. W. , Carslaw, K. S., Spracklen, D. V., Pringle, K. J., Merikanto, J., Korhonen, H. et al.. Intercomparison of modal and sectional aerosol microphysics representations within the same 3-D global chemical transport model, Atmos. Chem. Phys., 12, 4449–4476, 2012.

Marchand, M., Keckhut, P., Lefebvre, S., Claud, C., Cugnet, D., Hauchecorne, A., et al. (2012). Dynamical amplification of the stratospheric solar response simulated with the Chemistry-Climate Model LMDz-Reprobus. Journal of Atmospheric and Solar-Terrestrial Physics, 75–76, 147–160. https://doi.org/10.1016/j.jastp.2011.11.008

Mills, M. J., O. B. Toon, V. Vaida, P. E. Hintze, H. G. Kjaergaard, D. P. Schofield, and T. W. Robinson (2005), Photolysis of sulfuric acid vapor by visible light as a source of the polar stratospheric CN layer, J. Geophys. Res., 110, D08201, doi:10.1029/2004JD005519.

Mills, M. J., Schmidt, A., Easter, R., Solomon, S., Kinnison, D. E., Ghan, S. J., Neely, R. R., Marsh, D. R., Conley, A., Bardeen, C. G., and Gettelman, A.: Global volcanic aerosol properties derived from emissions, 1990–2014, using CESM1(WACCM), J. Geophys. Res.-Atmos., 121, 2332–2348, https://doi.org/10.1002/2015JD024290, 2016.

Mills, M. J., Richter, J. H., Tilmes, S., Kravitz, B., Mac-Martin, D. G., Glanville, A. A., Tribbia, J. J., Lamarque, J.-F., Vitt, F., Schmidt, A., Gettelman, A., Hannay, C., Bacmeister, J. T., and Kinnison, D. E.: Radiative and chemical response to interactive stratospheric sulfate aerosols in fully coupled CESM1(WACCM), J. Geophys. Res.-Atmos., 122, 13061–13078, https://doi.org/10.1002/2017JD027006, 2017.

Molod, A., Takacs, L., Suarez, M., and Bacmeister, J.: Development of the GEOS-5 atmospheric general circulation model: evolution from MERRA to MERRA2, Geosci. Model Dev., 8, 1339-1356, 10.5194/gmd-8-1339-2015, 2015.

Morgenstern, O., Braesicke, P. , O'Connor, F. M., Bushell, A. C., Johnson, C. E., Osprey, S. M. and Pyle, J. A. : Evaluation of the new UKCA climate-composition model – Part 1: The stratosphere, Geosci. Mod. Dev., 2, 43-57, https://doi.org/10.5194/gmd-2-43-2009, 2009.

Morgenstern, O., Hegglin, M. I., Rozanov, E., O'Connor, F. M., Abraham, N. L., Akiyoshi, H., ... & Zeng, G. (2017). Review of the global models used within phase 1 of the Chemistry–Climate Model Initiative (CCMI). *Geoscientific Model Development*, *10*(2), 639-671.

Mulcahy, J. P., Jones, C., Sellar, A., Johnson, B., Boutle, I. A., Jones, A., Andrews T. et al. Improved Aerosol Processes and Effective Radiative Forcing in HadGEM3 and UKESM1, Journal of Advances in Modeling Earth Systems, 10, 2786–2805. https://doi.org/10.1029/2018MS001464, 2018.

Mulcahy, J. P., Johnson, C., Jones, C. G., Povey, A. C., Scott, C. E., Sellar, A., Turnock, S. T. et al.: Description and evaluation of aerosol in UKESM1 and HadGEM3-GC3.1 CMIP6 historical simulations, Geosci. Model Dev., 13, 6383–6423, https://doi.org/10.5194/gmd-13-6383-2020, 2020.

Mulcahy, J. P., Jones, C. G., Rumbold, S. Kuhlbrodt, T., Dittus, A. J. Blockley, E. W. et al., : UKESM1.1: development and evaluation of an updated configuration of the UK Earth System Model, Geosci. Model Dev., 16, 1569–1600, https://doi.org/10.5194/gmd-16-1569-2023, 2023

Naujokat, B., An update of the observed Quasi-Biennial Oscillation of the stratospheric winds over the tropics, J. Atmos. Sci., 43, 1873 - 1877, https://doi.org/10.1175/1520-0469(1986)043<1873:AUOTOQ>2.0.CO;2, 1986.

Neely III, Ryan R. and Schmidt, Anja (2016) *VolcanEESM: Global volcanic sulphur dioxide (SO2) emissions database from 1850 to present.* Centre for Environmental Data Analysis. [Dataset] https://doi.org/10.5285/76ebdc0b-0eed-4f70-b89e-55e606bcd568

O'Connor, F. M., Johnson, C. E., Morgenstern, O., Abraham, N. L., Braesicke, P. et al.: Evaluation of the new UKCA climate-composition model– Part 2: The Troposphere, Geosci. Model Dev., 7, 41–91, https://doi.org/10.5194/gmd-7-41-2014, 2014.

O'Neill, B.C., Tebaldi, C., van Vuuren, D.P., et al., The Scenario Model Intercomparison Project (ScenarioMIP) for CMIP6. Geoscientific Model Development, 9, 9, 3461–3482, doi:10.5194/gmd-9-3461-2016, 2016.

Nielsen, J. E., Pawson, S., Molod, A., Auer, B., Da Silva, A. M., Douglass, A. R., ... & Wargan, K. (2017). Chemical mechanisms and their applications in the Goddard Earth Observing System (GEOS) earth system model. *Journal of Advances in Modeling Earth Systems*, *9*(8), 3019-3044.

Peuch, V.-H., Engelen, R., Rixen, M., Dee, D., Flemming, J., Suttie, M., Ades, M., Agusti-Panareda, A., Ananasso, C., Andersson, E., Armstrong, D., Barre, J., Bousserez, N., Dominguez, J. J., Garrigues, S., Inness, A., Jones, L., Kipling, Z., Letertre-Danczak, J.,

Parrington, M., Razinger, M., Ribas, R., Vermoote, S., Yang, X., Simmons, A., de Marcilla, J. G., and Thepaut, J.-N.: The Copernicus Atmosphere Monitoring Service: From Research to Operations, Bulletin of the American Meteorological Society, 103, E2650 – E2668, https://doi.org/10.1175/BAMS-D-21-0314.1, 2022.

Pringle, K. J., Tost, H., Message, S., Steil, B., Giannadaki, D., Nenes, A., Fountoukis, C., Stier, P., Vignati, E., and Lelieveld, J.: Description and evaluation of GMXe: a new aerosol submodel for global simulations (v1), Geosci. Model Dev., 3, 391–412, 2010.

Putman, W. M., & Lin, S. J. (2007). Finite-volume transport on various cubed-sphere grids. *Journal of Computational Physics*, *227*(1), 55-78.

Quaglia, I., Timmreck, C., Niemeier, U., Visioni, D., Pitari, G., Brodowsky, C., Brühl, C., Dhomse, S. S., Franke, H., Laakso, A., Mann, G. W., Rozanov, E., and Sukhodolov, T.: Interactive stratospheric aerosol models' response to different amounts and altitudes of SO2 injection during the 1991 Pinatubo eruption, Atmos. Chem. Phys., 23, 921–948, https://doi.org/10.5194/acp-23-921-2023, 2023.

Randel, W. J., Wang, X., Starr, J., Garcia, R. R., & Kinnison, D. (2024). Long-term temperature impacts of the Hunga volcanic eruption in the stratosphere and above. Geophysical Research Letters, 51, e2024GL111500. https://doi.org/10.1029/2024GL111500

Reinecker, M., Suarez, M., Todling, R., Bacmeister, J., Takacs, L., & Liu, H. (2008). The GEOS-5 data assimilation system-documentation of versions 5.0. 1, 5.1. 0 (No. NASA Tech Rep TM-2007, 104606).

Rémy, S., Kipling, Z., Huijnen, V., Flemming, J., Nabat, P., Michou, M., Ades, M., Engelen, R., and Peuch, V.-H.: Description and evaluation of the tropospheric aerosol scheme in the Integrated Forecasting System (IFS-AER, cycle 47R1) of ECMWF, Geoscientific Model Development, 15, 4881–4912, https://doi.org/10.5194/gmd-15-4881-2022, 2022.

Reynolds, R. W., N. A. Rayner, T. M. Smith, D. C. Stokes, and W. Wang, 2002: An Improved In Situ and Satellite SST Analysis for Climate. J. Climate, 15, 1609–1625, https://doi.org/10.1175/1520-0442(2002)015<1609:AIISAS>2.0.CO;2.

Schallock, J., C. Brühl, C. Bingen, M. Höpfner, L. Rieger, and J. Lelieveld (2023), Reconstructing volcanic radiative forcing since 1990, using a comprehensive emission inventory and spatially resolved sulfur injections from satellite data in a chemistry-climate model, Atmos. Chem. Phys., 23, 1169–1207.

Scinocca, J. F.: An Accurate Spectral Non-Orographic Gravity Wave Parameterization for General Circulation Models, J. Atmos. Sci., 60, 667–682, https://doi.org/10.1175/1520-0469(2003)060%3C0667:AASNGW%3E2.0.CO;2, 2003.

Scinocca, J. F., McFarlane, N. A., Lazare, M, Li, J., and Plummer, D., Technical Note: The CCCma third generation AGCM and its extension into the middle atmosphere, Atmos. Chem. Phys., 8, 7055–7074, https://doi.org/10.5194/acp-8-7055-2008, 2008.

Seddon, J., Stephens, A., Mizielinski, M. S., Vidale, P. L., and Roberts, M. J.: Technology to aid the analysis of large-volume multi-institute climate model output at a central analysis

facility (PRIMAVERA Data Management Tool V2.10), Geosci. Model Dev., 16, 6689–6700, https://doi.org/10.5194/gmd-16-6689-2023, 2023.

Sekiya, T., K. Sudo, and T. Nagai (2016), Evolution of stratospheric sulfate aerosol from the 1991 Pinatubo eruption: Roles of aerosol microphysical processes, J. Geophys. Res. Atmos., 121, 2911–2938, doi:10.1002/2015JD024313.

Sellar, A., J., C. G. Jones, J. Mulcahy, Y. Tang et al. (2019), UKESM1: Description and Evaluation of the U.K. Earth System Model, J. Adv. Mod. Earth Systems, 11, 4513-4558, https://doi.org/10.1029/2019MS001739

Sellar, A., J. Walton, C. G. Jones, R. Wood et al. (2020), Implementation of U.K. Earth System Models for CMIP6, J. Adv. Mod. Earth Systems, 12, e2019MS001946. https://doi.org/10.1029/2019MS001946

Strahan, S. E., Duncan, B. N., & Hoor, P. (2007). Observationally derived transport diagnostics for the lowermost stratosphere and their application to the GMI chemistry and transport model. *Atmospheric Chemistry and Physics*, *7*(9), 2435-2445.

Sukhodolov, T., Egorova, T., Stenke, A., Ball, W. T., Brodowsky, C., Chiodo, G., Feinberg, A., Friedel, M., Karagodin-Doyennel, A., Peter, T., Sedlacek, J., Vattioni, S., and Rozanov, E.: Atmosphere ocean aerosol chemistry climate model SOCOLv4.0: description and evaluation, Geosci. Model Dev., 14, 5525–5560, https://doi.org/10.5194/gmd-14-5525-2021 , 2021.

Taha, G., et al. (2021), OMPS LP Version 2.0 multi-wavelength aerosol extinction coefficient retrieval algorithm, Atmospheric Measurement Techniques, 14, https://doi.org/10.5194/amt-14-1015-2021

Taha, G., et al. "Tracking the 2022 Hunga Tonga-Hunga Ha'apai aerosol cloud in the upper and middle stratosphere using space-based observations." Geophysical Research Letters 49.19 (2022): e2022GL100091.

Tilmes, S., Mills, M. J., Zhu, Y., Bardeen, C. G., Vitt, F., Yu, P., Fillmore, D., Liu, X., Toon, B., and Deshler, T.: Description and performance of a sectional aerosol microphysical model in the Community Earth System Model (CESM2), Geosci. Model Dev., 16, 6087-6125, 10.5194/gmd-16-6087-2023, 2023. doi: 10.5194/gmd-16-6087-2023

Tatebe, H., Ogura, T., Nitta, T., Komuro, Y., Ogochi, K., Takemura, T., Sudo, K., Sekiguchi, M., Abe, M., Saito, F., Chikira, M., Watanabe, S., Mori, M., Hirota, N., Kawatani, Y., Mochizuki, T., Yoshimura, K., Takata, K., O'ishi, R., Yamazaki, D., Suzuki, T., Kurogi, M., Kataoka, T., Watanabe, M., and Kimoto, M.: Description and basic evaluation of simulated mean state, internal variability, and climate sensitivity in MIROC6, Geosci. Model Dev., 12, 2727–2765, https://doi.org/10.5194/gmd-12-2727-2019, 2019.

Telford, P., Braesicke, P., Morgenstern, O. and Pyle, J. : Technical Note: Description and assessment of a nudged version of the new dynamics Unified Model, Atmos. Chem. Phys., 8, 1701–1712, https://doi.org/10.5194/acp-8-1701-2008, 2008.

1255   Telford, P., Braesicke, P., Morgenstern, O. and Pyle, J. : Reassessment of causes of ozone
1256   column variability following the eruption of Mount Pinatubo using a nudged CCM, Atmos.
1257   Chem. Phys., 9, 4251–4260, https://doi.org/10.5194/acp-9-4251-2009, 2009.

1258   Tsujino, H. et al. JRA-55 based surface dataset for driving ocean–sea-ice models (JRA55-do).
1259   Ocean Modell. 130, 79–139 (2018).

1260   Thomason, L. W., N. Ernest, L. Millán, L. Rieger, A. Bourassa, J.-P. Vernier, G. Manney, T.
1261   Peter, B. Luo, and F. Arfeuille (2018), A global, space-based stratospheric aerosol
1262   climatology: 1979 to 2016, Earth System Science Data, 10, 469–492,
1263   https://doi.org/10.5194/essd-10-469-2018.

1264   Vehkamäki, H., Kulmala, M., Napari, I., Lehtinen, K. E., Timmreck, C., Noppel, M., and
1265   Laaksonen, A.: An improved parameterization for sulfuric acid-water nucleation rates for
1266   tropospheric and stratospheric conditions, J. Geophys. Res.-Atmos., 107, AAC 3- 1–AAC
1267   3-10, https://doi.org/10.1029/2002JD002184, 2002.

1268   Walters, D., Baran, A. J. Boutle, I., Brooks, M., Earnshaw, P., Edwards, J., Furtado, K., Hill, P.
1269   et al. The Met Office Unified Model Global Atmosphere 7.0/7.1 and JULES Global Land
1270   7.0 configurations, Geosci. Model Dev., 12, 1909–1963, 2019.

1271   Wang, X., Randel, W., Zhu, Y., Tilmes, S., Starr, J., Yu, W., et al. (2023). Stratospheric climate
1272   anomalies and ozone loss caused by the Hunga Tonga-Hunga Ha'apai volcanic eruption.
1273   Journal of Geophysical Research: Atmospheres, 128, e2023JD039480.
1274   https://doi.org/10.1029/2023JD039480

1275   Watanabe, S., Hajima, T., Sudo, K., Nagashima, T., Takemura, T., Okajima, H., Nozawa, T.,
1276   Kawase, H., Abe, M., Yokohata, T., Ise, T., Sato, H., Kato, E., Takata, K., Emori, S., and
1277   Kawamiya, M.: MIROC-ESM 2010: model description and basic results of CMIP5-20c3m
1278   experiments, Geosci. Model Dev., 4, 845–872, https://doi.org/10.5194/gmd-4-845-2011,
1279   2011.

1280   Williams K. D., Copsey, D., Blockley, E.W., Bodas-Salcedo, A., Calvert, D., Comer, R., et al.
1281   (2018). The Met Office Global Coupled Model 3.0 and 3.1 (GC3.0 and GC3.1)
1282   Configurations. Journal of Advances in Modeling Earth Systems, 10(2), 357–380.
1283   https://doi.org/10.1002/2017MS001115 (2018)

1284   Williams, J. E., Huijnen, V., Bouarar, I., Meziane, M., Schreurs, T., Pelletier, S., Marecal, V.,
1285   Josse, B., and Flemming, J.: Regional evaluation of the performance of the global CAMS
1286   chemical modeling system over the United States (IFS cycle 47r1), Geoscientific Model
1287   Development, 15, 4657–4687, https://doi.org/10.5194/gmd-15-4657-2022, 2022.

1288   Wood, N., Staniforth, A., White, A., Allen, T., Diamantakis, M., Gross, M., Melvin, T., Smith,
1289   C., Vosper, S., Zerroukat, M., and Thuburn, J.: An inherently mass-conserving semi-
1290   implicit semi-Lagrangian discretization of the deep-atmosphere global nonhydrostatic
1291   equations, Q. J. Roy. Meteorol. Soc., 140, 1505–1520, https://doi.org/10.1002/qj.2235,
1292   2014.

1293   Yu, P., O. B. Toon, C. G. Bardeen, M. J. Mills, T. Fan, J. M. English, and R. R. Neely (2015),
1294   Evaluations of tropospheric aerosol properties simulated by the community earth system

model with a sectional aerosol microphysics scheme, J. Adv. Model. Earth Syst., 7, 865–914, doi:10.1002/2014MS000421.

Yu, W., Garcia, R., Yue, J., Smith, A., Wang, X., Randel, W., ... & Mlynczak, M. (2023). Mesospheric temperature and circulation response to the Hunga Tonga-Hunga-Ha'apai volcanic eruption. Journal of Geophysical Research: Atmospheres, 128(21), e2023JD039636.

Zhang, J., Kinnison, D., Zhu, Y., Wang, X., Tilmes, S., Dube, K., & Randel, W. (2024). Chemistry contribution to stratospheric ozone depletion after the unprecedented water-rich Hunga Tonga eruption. Geophysical Research Letters, 51, e2023GL105762. https://doi.org/10.1029/2023GL105762

Zhou, X., S.S. Dhomse, W. Feng, G. Mann, S. Heddell, H. Pumphrey, B.J. Kerridge, B. Latter, R. Siddans, L. Ventress, R. Querel, P. Smale, E. Asher, E.G. Hall, S. Bekki and M.P. Chipperfield (2024), Antarctic vortex dehydration in 2023 as a substantial removal pathway for Hunga Tonga-Hunga Ha'apai water vapour, Geophysical Research Letters, 51, e2023GL107630, doi:10.1029/2023GL107630.

Zhu, Y., Bardeen, C.G., Tilmes, S. et al. Perturbations in stratospheric aerosol evolution due to the water-rich plume of the 2022 Hunga-Tonga eruption. Commun Earth Environ 3, 248 (2022). https://doi.org/10.1038/s43247-022-00580-w